SPR-Part B
MD-21-SHA/UM/5-12

MARYLAND DEPARTMENT OF TRANSPORTATION
STATE HIGHWAY ADMINISTRATION

RESEARCH REPORT

An Integrated Intelligent Intersection Control System (III-CS) for Safety Improvement and Delay Minimization

GANG-LEN CHANG, YEN-HSIANG CHEN, YAO CHENG

UNIVERSITY OF MARYLAND, COLLEGE PARK

FINAL REPORT

January 2022

This material is based upon work supported by the Federal Highway Administration under the State Planning and Research program. Any opinions, findings, and conclusions or recommendations expressed in this publication are those of the author(s) and do not necessarily reflect the views of the Federal Highway Administration or the Maryland Department of Transportation. This report does not constitute a standard, specification, or regulation.

TECHNICAL REPORT DOCUMENTATION PAGE

1. Report No. MD-21-SHA/UM/5-12	**2. Government Accession No.**	**3. Recipient's Catalog No.**
4. Title and Subtitle An Integrated Intelligent Intersection Control System (III-CS) for Safety Improvement and Delay Minimization		**5. Report Date** January 2022 .
		6. Performing Organization Code
7. Author(s) Gang-Len Chang, Yen-Hsiang Chen, Yao Cheng		**8. Performing Organization Report No.**
9. Performing Organization Name and Address The University of Maryland, College Park, MD 20742		**10. Work Unit No.**
		11. Contract or Grant No. SHA/UM/5-12 SP910B4K
12. Sponsoring Agency Name and Address Maryland Department of Transportation (SPR) State Highway Administration Office of Policy & Research 707 North Calvert Street Baltimore MD 21202		**13. Type of Report and Period Covered** SPR-B Final Report (December 12, 2018 – December 31, 2021)
		14. Sponsoring Agency Code (7120) STMD - MDOT/SHA
15. Supplementary Notes		

16. Abstract

The primary objectives of this research are to develop and test an ***I**ntegrated **I**ntelligent **I**ntersection **C**ontrol **S**ystem (III-CS)* that can concurrently address both safety and efficiency issues. Based on the dilemma zone protection system (DZPS) developed jointly by MDOT SHA and the research team, the proposed III-CS will have the following key features: execute the optimal green termination algorithm under the actuated control function to concurrently minimize the likelihood of rear-end collisions and total traffic delay; and activate the all-red extension to prevent potential angled crashes when detecting red-light running vehicles. From in-depth analysis results of two field studies two months apart, the deployed III-CS has proved its effectiveness in preventing angled crashes with its perfect detection rate, optimally activating or terminating the green extension, and significantly reducing the number of vehicles trapped in the dilemma zone, which is the main contributing factor to rear-end collisions.

17. Key Words Dilemma zone, all-red extension, actuated signal control, intersection safety, dynamic green extension	**18. Distribution Statement** This document is available from the Research Division upon request.

19. Security Classif. (of this report) None	**20. Security Classif. (of this page)** None	**21. No. of Pages**	**22. Price**

Form DOT F 1700.7 (8-72) Reproduction of completed page authorized

Table of Contents

List of Figures

List of Tables

Chapter 1: Introduction

1.1 Research background

Most accidents occurring at suburban high-speed intersections are either rear-end collisions or angled crashes. Over the past several years, the intersection dilemma zone protection system (DZPS), developed collectively by the **M**aryland **D**epartment of **T**ransportation, **S**tate **H**ighway **A**dministration (MDOT SHA) and the ATTAP (**A**pplied **T**echnology and **T**raffic **A**nalysis **P**rogram) research team, has demonstrated its effectiveness in preventing angled crashes caused mainly by red-light running vehicles. However, the system's impact on factors contributing to rear-end collisions is passive and indirect in nature. This is because drivers approaching the intersection may not observe the presence of the DZPS's detection camera and, in turn, do not take reactive actions such as slowing their speed, especially during the yellow phase.

Theoretically, the likelihood of rear-end collisions could be minimized if drivers were willing to slow their speeds when approaching an intersection or follow traffic guidelines to avoid being trapped in a dilemma zone during the yellow phase. One such strategy reported in the literature is to dynamically extend the green time with a conventional actuated signal controller. However, because of the point-measurement nature of the actuated control's detector, this type of green-extension strategy cannot precisely detect the number of vehicles trapped in the dilemma zone and their approaching speeds. In addition, the execution of a green extension or termination with the "gap-out" threshold has not yielded the expected level of performance, and thus remains at the project demonstration level.

In contrast, the DZPS deployed by MDOT SHA is capable of detecting both the temporal and spatial evolution of approaching vehicles' speeds and locations in the monitoring zone (about 1000 ft) at the interval of 0.1 second through a long-range sensor. One can take advantage of such valuable information to identify the optimal gap for green termination (before reaching the specified maximum green) so that all vehicles will be able to stop smoothly when the signal is changing to a yellow phase. As such, an intersection deployed with DZPS can certainly be enhanced to offer a proactive function to prevent potential rear-end collisions if its actuated signal controller is properly programmed to convert from the standard "gap-out" control to the optimal

green-termination algorithm, based on real-time detected spatial evolution of approaching vehicles.

Depending on the spatial distribution of the arriving vehicle pattern during the yellow phase, the type of algorithms designed for the green-termination may identify multiple gaps from the perspective of preventing rear-end collisions. To advance the DZPS to proactively prevent rear-end collisions, one can further extend the system's decision function to identify the optimal gap from those that satisfy the safety criteria in order to concurrently minimize the total vehicle delay due to the phase transition.

Moreover, the real-time data of all approaching vehicles' time-varying speeds and locations during different signal phases, available from the DZPS's long-range sensor, also allows its users to calibrate reliable algorithms for estimating the time-varying queue distance during each cycle and the residual queues at the onset of a green phase. Such information, if provided to the approaching vehicles via some effective communication infrastructure, can further reduce the likelihood of more vehicles joining the residual queues, and thus minimizing their experienced delays at the target intersection. With its functionality enhanced, the DZPS deployed by MDOT SHA would be capable of providing full safety protection to drivers at the desirable level of operational efficiency.

1.2 Research objectives

The primary objectives of this research are to develop and test an ***I**ntegrated **I**ntelligent **I**ntersection **C**ontrol **S**ystem (III-CS)* that can concurrently address both safety and efficiency issues. Based on the dilemma zone protection system (DZPS) developed jointly by MDOT SHA and the research team, the proposed III-CS will have the following key features:

- Execute the optimal green termination algorithm under the actuated control function to concurrently minimize the likelihood of rear-end collisions and total traffic delay; and
- Activate the all-red extension to prevent potential angled crashes when detecting red-light running vehicles.

In addition, all deployed III-CS will have the ability to link together to create a service network, allowing SHA engineers to monitor their performance through real-time detected traffic data (e.g., the distributions of speeds, headways, flow rate), and to conduct off-line safety analysis, including accident records, near-crash frequency, and impacts on the behaviors of driving populations over each intersection deployed with the proposed III-CS.

1.3 Report Organization

To accomplish the research objectives, the project is divided into three parts: 1.) theoretical development of several control algorithms; 2.) integration of the developed algorithms with existing DZPS and intersection signals for field deployment; and 3.) benefit assessment of the developed *III-CS* before and after its field deployment. These actions, along with key research results and empirical findings, are reported in the following five chapters:

Chapter 2 provides an overview of the developed III-CS's key components and their primary functions. This will include two wide-range sensors for tracking the temporal and spatial evolution of all vehicles within the target detection zone; a customized computing device installed in the signal controller to house the two control algorithms for preventing rear-end collisions and angled crashes; and a real-time monitor for remote assessment of the deployed system's performance and execution of any necessary parameter adjustments.

Chapter 3 discusses two new control algorithms developed to prevent rear-end collisions at high-speed intersections, sharing the same hardware for the Dynamic All-Red Extension (DARE) system. Algorithm1 is extended from the state-of-the-practice "gap out" control logic that is relatively straightforward for comprehension and implementation. Algorithm 2 is a more sophisticated control logic that can dynamically extend the green duration based on the projected speeds and locations of vehicles within the detected zone, and by the risk of incurring rear-end collisions if the green phase is terminated at any time point over the next pre-specified time horizon. A detailed description of the core logic, parameters, and operational procedures associated with each of these two control algorithms for preventing rear-end collisions under actuated signal control is provided in this chapter.

Chapter 4 presents the procedures and results of the pre-deployment assessment of the integrated intelligent intersection control system (III-CS) at three candidate intersections. The pre-deployment assessment aims to estimate the risk of rear-end collisions and angle crashes for current driving populations, using a simulation analysis where key parameters are calibrated from the target intersection's field data; the simulator can replicate the candidate intersection's current traffic patterns and driving behaviors. The risk level revealed by the simulator will serve as the basis for assessing the potential effectiveness and benefits of the III-CS developed in this project.

Chapter 5 provides the assessment results from two after-deployment field studies, focusing on the III-CS's effectiveness with respect to its timely activation of a dynamic all-red extension function to prevent angled crashes; dynamic extension of the green phase to minimize the number of vehicles trapped in the dilemma zone during the yellow phase; and potential long-term impacts on the behaviors of driving populations, especially in the reduction of high-speed drivers and red-light runners. Also included in this chapter is the time-varying impacts of the deployed system on the traffic patterns and behaviors of driving populations.

Chapter 6 summarizes the research findings from this study, including valuable lessons for future deployment of the developed III-CS at different intersections. The need for extending the current system's functions to tackle collisions between turning and through vehicles under various signal design plans are also discussed in this chapter.

Chapter 2: System Design Features

2.1 Related studies in Dilemma Zone protection

Despite sustained investment in traffic safety by both federal and state transportation agencies over the past several decades, how to effectively minimize intersection accidents remains a critical yet challenging task. According to the statistics by NHTSA (2019), intersection and related crashes constitute 28.8% of the 52,645 total fatal crashes in 2017; around 70% of such are either rear-end collisions or angled crashes (AASHTO, 2010).

The statewide accident statistics for Maryland from 2015 to 2019 reveal the same pattern, with 32.8 percent of the 177,477 crashes occurring at intersections (Maryland State Police, 2019). Traffic safety professionals have devoted immense effort over the years to investigating factors contributing to such crashes. Various countermeasures for safety improvement have been proposed, including driver education (NHTSA, 2009), geometric improvements (e.g., Wang and Abdel-Aty, 2019; Wood and Donnell, 2016), deployment of monitoring devices (e.g., red-light camera), and design of signal control strategies with embedded safety functions (e.g., Webster and Ellson, 1965; Parsonson et al., 1974; Zegeer and Deen, 1978; Parsonson et al., 1979; Peterson et al., 1986; Vincent and Peirce, 1988; Kronborg and Davidsson, 1993; Bonneson & Mccoy, 1996; Kronborg et al., 1997; Kronborg et al., 1997; Bonneson et al., 2002; Zimmerman, 2007; Tarko et al., 2006; Zimmerman et al., 2012; and Park et al., 2016).

The system developed in this study, an **I**ntegrated **I**ntelligent **I**ntersection **C**ontrol **S**ystem (III-CS), falls into the last category of countermeasures and focuses on advancing the existing practice of actuated signal control with safety-oriented dynamic algorithms that can minimize the risk of incurring rear-end collisions between vehicles during both the “gap-out” and “max-out” of the green phase. More specifically, it is designed with the notion of minimizing any additional hardware and computation so that the entire system can be deployed at existing actuated-control intersections with minimal additional costs.

The proposed system for preventing rear-end crashes at signalized intersections is grounded in state-of-the-art studies in traffic safety, especially in the following two areas: driver behavior and contributing factors that collectively cause crashes; and various control strategies

designed to minimize drivers from encountering such hazardous scenarios. In review of the related literature in the former area, it is noticeable that rear-end collisions are most commonly incurred due to inconsistent "pass-or-stop" decisions between the leading and following vehicles during the signal phase transition from green to yellow. Although there are various factors that may contribute to such inconsistent decisions (e.g., Chang et al., 1985; Zimmerman and Bonneson, 2004; Gates et al., 2007; Chiou et al., 2010; Liu et al., 2011), drivers trapped within their "indecision zones" or "dilemma zones" are generally viewed as the primary contributor.

A pioneering study on this subject by Gazis et al. (1960) first presented the concept of the "Type-I dilemma zone," defined as the range of distance from the intersection in which drivers can neither stop comfortably nor pass safely during phase transitions. Addressing the same concern, Parsonson et al. (1974) proposed the notion of the "Type-II dilemma zone" to indicate the spatial distribution in which those drivers have the probability of between 10% to 90% to make the stop decision during the yellow phase.

Along this line, some researchers have further investigated the interrelations of such a dilemma zone and its contributing factors, including the distributions of approaching speeds, distances to the intersection, driver characteristics, and responses to the phase transition. For instance, Sheffi and Mahmassani (1981) first investigated the behaviors of drivers in response to the phase transition from the field data and then formulated their "stop-or-pass" decision during the yellow phase with a binary discrete-choice model. Liu et al. (2011) conducted field observations of 1,123 drivers' responses at signalized intersections and identified a list of critical factors (e.g., approaching speed, volume, gender, vehicle type, etc.) that may affect a driver's decision and the formation of the resulting dilemma zone. Gates et al. (2007) further empirically studied the same driver decision issue by analyzing the distribution of brake-response times, deceleration rates, estimate time to the stop lines, and adjacent vehicles' decisions in addition to the yellow phase duration.

Consistent with the findings by Liu et al. (2011), Papaioannou (2007) reported that both gender and age are critical factors affecting a driver's response to the yellow phase. The most recent empirical study, conducted at 87 intersections by Savolainen et al. (2016), further confirmed

the significance of such vital decisions and those dilemma-zone related factors reported in the literature, including speed limits, yellow phase ratio, all-red interval, red-light camera, and the setting of advanced warning signs. Further discussion on the two types of dilemma zones have been reported in the study by Urbanik and Koonce (2007).

Some recent studies on this aspect focused on estimating the probability for drivers to take the stop-action under various scenarios and the resulting distribution of dilemma zones. Examples of such work include the research by Hurwitz et al. (2010; 2012), who employed the fuzzy set to model driver decisions in the indecision zone and to account for their perception imprecision with respect to the speed and distance to the intersection. Elhenawy et al. (2015) surveyed the probability of drivers taking a stop decision during the yellow phase under a controlled experimental environment and reported the effectiveness of using the discrete choice model and the Support Vector Machine method (Hastie et al., 2009) to improve the prediction results.

Grounded in the findings of factors associated with driver decisions within the dilemma zone, some researchers have devoted their work to designing control strategies that prevent drivers from being trapped in such a hazardous zone and thus incurring a rear-end collision. Most strategies under the actuated signal control focus on how to extend the green time when the signal is ready to "gap-out" or "max-out" by detecting the presence of vehicles within the intersection's dilemma zone. Examples of these studies range from the earliest design of a green extension by Webster and Ellson (1965) to a similar but more extensive study by Zegeer and Deen (1978).

With the same design notion, Tarko et al. (2006) introduced a probabilistic approach to predict and prevent vehicles from being trapped in the dilemma zone with a green extension after max-out, unless it is exceeding the preset maximal extension. Bonneson et al. (2002) proposed to divide the green duration into two stages, where its first stage of control does not allow any vehicle to be within the dilemma zone when executing the gap-out but can grant an extension for the presence of one vehicle during the second stage of green. Zimmerman (2007) proposed an extension of an additional green phase for 1.5 seconds for a detected truck during the gap-out to accommodate their unique operational characteristics (e.g., longer stopping distance, less willing to stop, and more likely to run over the red-light phase). Most field evaluations of dilemma-zone

protection systems designed with the aforementioned control algorithms have confirmed their effectiveness in reducing intersection crashes (e.g., Abbas et al., 2016).

The dynamic all-red extension (DARE) is another type of intersection control strategy that has been reported in Phase I of this project. Most angled crashes at signalized intersections can be effectively reduced by extending the all-red clearance interval when predicting or detecting red-light runners in real time. A large body of systems designed to prevent such angled crashes has been reported in the safety literature.

For example, LHOVRA (Peterson et al., 1986; Kronborg and Davidsson, 1993) is an adaptive signal system that will activate a green extension at the first stage to protect roadway users; if the green extension exceeds the preset maximum green duration, then the system will activate DARE. By installing a series of loop detectors (at least four per lane) or a single microwave detector, the "speed discrimination" signal system by Baguley and Ray (1989) was designed to offer a green extension when detecting vehicles in the dilemma zone. The system will then activate DARE after extending to the maximum allowable extension. With extensive simulation experiments, Archer and Young (2019) have evaluated the effectiveness of different strategies for minimizing angled crashes, including green extension, amber extension, DARE, and their combinations. Li et al. (2018) have explored the potential benefits of operating the DARE under connected vehicle (CV) environments and concluded that DARE's false alarm rate can be reduced significantly.

Although DARE is conceptually intuitive and has been extensively implemented in European countries for decades, its potential in safety improvements within the U.S. has been constrained by state of the practice guided by the *MUTCD 2003* (Gates and Noyce, 2016). In Section 4D.10 of *MUTCD 2003* (FHWA, 2003), it states that *"The duration of a red clearance interval shall be predetermined,"* which forbids any changes with the red interval. In response to such a constraint, some proposed to preset a longer clearance time which, however, may achieve only a short-term safety improvement, but a diminished long-run effectiveness since drivers are likely to be more aggressive after noticing such a change (Souleyrette et al., 2004). Presetting a

longer all-red clearance time also increases the intersection's loss time without the presence of red-light runners.

The later version of MUTCD 2009 (FHWA, 2009) offers a new guideline in its Section 4D.26. It states that "When used, the duration of the red clearance interval shall be determined using engineering practices," opening the door for implementing DARE to improve safety while preserving the operational efficiency of the intersections. As a result, theoretical developments and field implementations with respect to various DARE designs have emerged in the past decade. For example, Zhang et al. (2011; 2012) proposed different probabilistic modeling methods to concurrently reduce the false alarm and detection rates. Simpson et al. (2017) also confirmed DARE's effectiveness with data from three years of field implementation at nine signalized intersections in North Carolina.

Using the Empirical-Bayes method from the data of eight intersections in Oregon, Olson (2012) also reported a 36% reduction in crash frequency with a well-designed DARE. Along the same line but with hardware-in-the-loop simulations, Hurwitz et al. (2016) concluded that no additional delay would be incurred with DARE and Adabi et al. (2017) also confirmed the expected safety improvements with such a design even with different control strategies. It has also been reported that DARE's effectiveness can be further enhanced with the radar sensors' extended coverage (e.g., Park et al., 2016; 2018).

In recent decades, the advance of adaptive control technologies has enabled traffic researchers to address safety issues due to the presence of dilemma zones from multiple avenues. An example can be found in a series of studies by those researchers for LHOVRA (Peterson et al., 1986; Kronborg and Davidsson, 1993), who proposed to concurrently contend with rear-end collisions and red-light running with a green extension, variable yellow duration, dynamic red-phase clearance, and skipping and/or reverting phase sequence (Peterson et al., 1986; Kronborg and Davidsson, 1993). An enhanced version of LHOVRA, named Self Optimizing Signal control (SOS), has been further enhanced to concurrently tackle the intersection delay and safety issues with an advanced adaptive signal controller and algorithm (Kronborg et al., 1997). Developed independently but with similar system features, Microprocessor Optimized Vehicle Actuation

(MOVA) is also capable of accounting for delay minimization with its embedded dynamic gap-checking function when making the decision of green extension to preventing potential crashes (Kronborg and Davidsson, 1993; Vincent and Peirce, 1988).

To concurrently address both safety and delay issues, Sharma et al. (2007; 2016) innovatively applied the hazard function method to convert the design of signal timing strategies as a cost-benefit issue, based on the estimated probability of traffic movement conflicts. Their proposed models, if implemented properly in an adaptive control environment, offer the potential to account for the delay and safety on both the primary arterial and side streets.

With the above literature reviews, one shall notice that most systems with real-time adaptive control infrastructure can certainly offer more powerful and extensive functions to address rear-end and angled crash issues at intersections, but inevitably at costs (e.g., hardware, operating, and maintenance) much higher than the popular actuated signal control system. The required high system reliability and data precision—as well as quality for executing such adaptive control designs—often demands prohibitive maintenance and operating costs from the responsible state or local highway agencies. As such, most adaptive systems for concurrently tackling intersection safety and delay issues, despite their potential effectiveness, have been deployed mainly at the project demonstration level, but not in practice.

2.2 Description of key system features

Fig. 2.1 shows the key components of the *Integrated Intelligent Intersection Control System (III-CS)*, which is designed to execute its embedded functions for preventing rear-end collisions and angled crashes with an actuated controller. This system utilizes the same hardware and communication devices deployed in the previous phase, a Dilemma Zone Protection System (DZPS) (Park et al., 2016; Park et al., 2018), but provides two new control algorithms and one remote-monitoring module. Its main function is to extend the DZPS from preventing angle crashes to minimizing the likelihood of having rear-end collisions during the phase transition. The entire III-CS comprises the following key components:

- **Wide-range vehicle sensors**: The long-range microwave detectors are deployed to track the speed evolution of each vehicle within the detection zone from the stop line to the upper bound (600-1000 ft), based on the spatial distribution of dilemma zones computed from the behaviors of the driving population when they approach the target intersection. As shown in Figure 2-2, such a sensor shall be capable of tracking all vehicles within the identified detection zone and computing each of their time-varying speeds, distances, and expected times to reach the intersection's stop line at an interval less than 0.15 seconds.

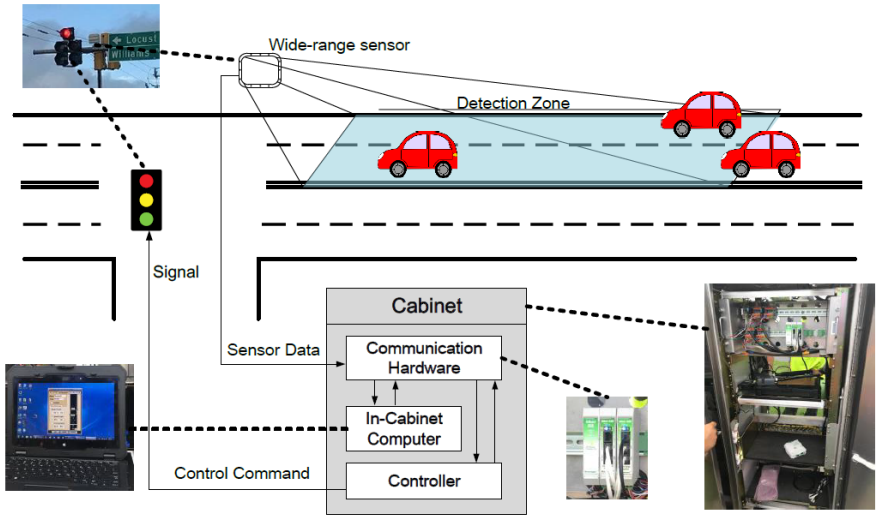

Figure 2-1: Key components of the developed Integrated Intelligent Intersection Control System.

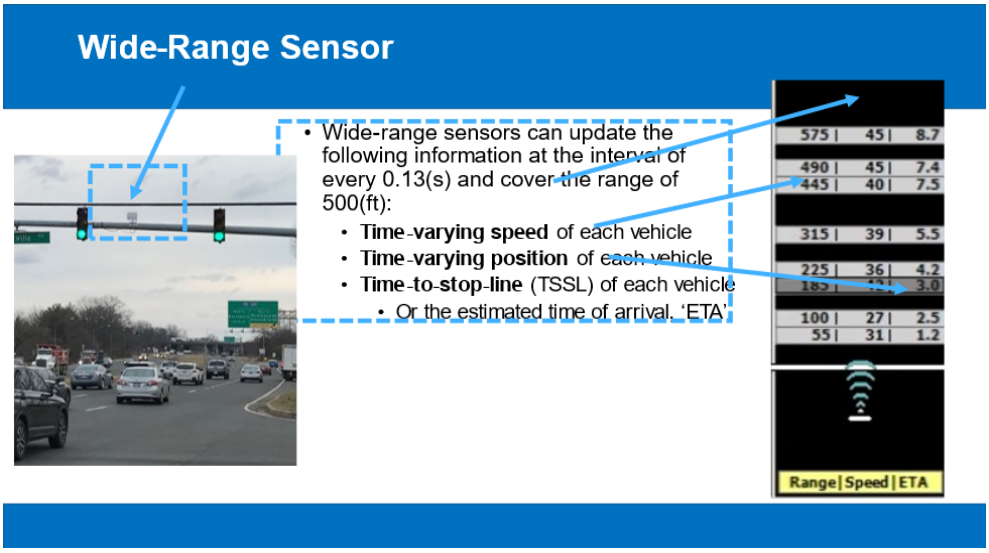

Figure 2-2: A graphical illustration of the wide-range sensor's functions and its field deployment.

- **Intersection signal controller**: The signal controller provides the signal phase and timing (SPaT) data to the in-cabinet computer and receives the instructions for either extending the green interval or executing the all-red extension if triggered by the sensor. Note that controllers in the developed *Integrated Intelligent Intersection Control System (III-CS)* shall be capable of offering two types of all-red interval: one for normal operations between phase transition and the other for reacting to detected red-light runners. For example, when the signal is in a yellow phase after reaching the maximum green duration, the developed system will identify vehicles approaching in the monitoring zone with their speeds and locations, and calculate the probability of whether or not a detected vehicle will take the ‘‘pass’’ decision during the yellow and all-red phases.
- **In-cabinet computer:** The intelligence of such an Integrated Intelligent Intersection Control System *(III-CS)* resides in its in-cabinet computer, which serves to exercise the following critical functions in real time: receiving traffic data from the wide-range detector(s); executing the algorithm to project the detected vehicles' evolution patterns; assessing the risk of incurring rear-end collisions between detected vehicles; and executing the action plan from the decision model by sending the instructions of either green extension or all-red extension to the responsible intersection controller. Figure 2-3 illustrates the operational flowchart and key logic of the dynamic all-red extension algorithm embedded in the in-cabinet computer; Figure 2-4 highlights the core logic of the other embedded algorithm for dynamic green extension.

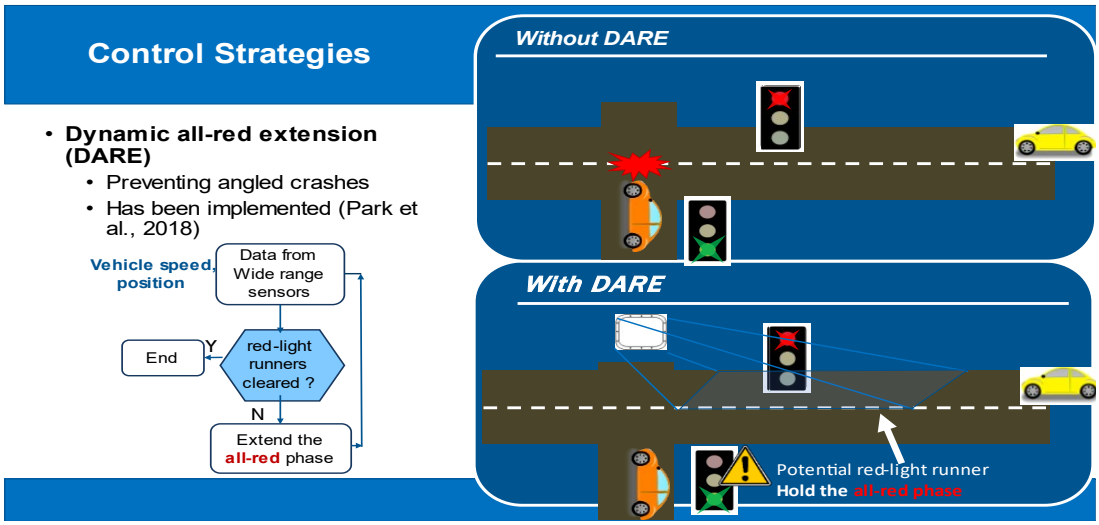

Figure 2-3: The algorithm for dynamic all-red extension embedded in the in-cabinet computer.

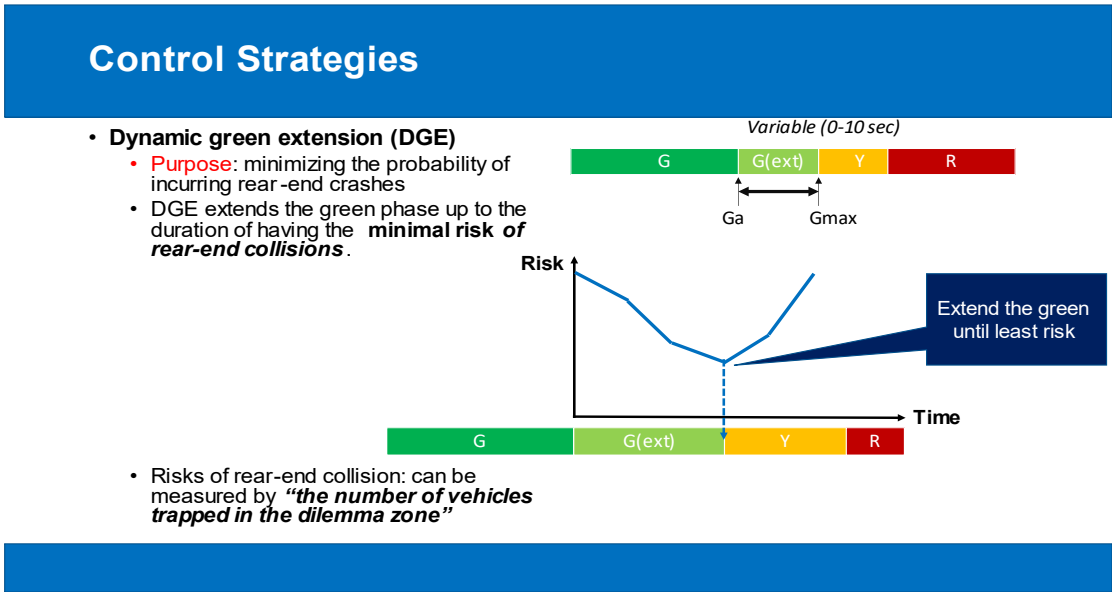

Figure 2-4: The algorithm for dynamic green-time extension in the in-cabinet computer

- **A real-time remote monitor:** This specially designed monitor is developed to facilitate traffic engineers' real-time monitoring of the deployed system's performance and the real-time detected traffic conditions, including the speeds of all detected vehicles, time-varying queue length, and the number of vehicles within the dilemma zone. Table 2-1 shows the list of key devices for such a remote real-time monitor. Figure 2-5 displays an example of the queue length monitoring with the developed monitor.

Table 2-1: List of key devices for the remote system monitor

Laptop	2 (1 in cabinet; 1 is used to connect)
Power Cables of Laptops	2
USB-to-RJ11(landline) B+B "Smartworx" **Landline to USB Converter** 	2 + a few (in case some of the converters are not working)
Verizon Modem (Sierra RV-50)	2 (1 for in-cabinet computer 1 for laptop outside)
Ethernet Splitter	1
Antennas of Modem	**4 (2 for each modem)**
Power Cable of Modem	2
Ethernet Line (laptop to Modem)	2
Portable Wi-Fi	0 + 1 (as backup)
Safety Vest	2 (depends on # crew)
Extension Cord **(power for antenna)**	2
Laptop Lock & Chain	1
Zip Ties (to be used together with lock & chain)	many as needed

Note that this function for queue monitoring is set in channel 8 of the signal controller, because channels 1- 4 are reserved for real-time control operations. The entire detection zone of 750 ft, as shown in Figure 2-5, is divided into four segments (i.e., Alerts 1-4), each containing four sub-detection zones. The vehicles at each sub-zone will be converted into time-varying queues and transmitted to the real-time monitor via channel 8 of the signal controller.

Figure 2-6 shows an example of detected time-dependent queue length at the MD 4 at Forestville Rd. displayed in the real-time monitor. An example of detected vehicle speeds by the wide-range sensor and displayed from the remote monitor is shown in Figure 2-7. Figure 2-8 provides a graphical display of the queue length detection within each subzone in Channel 8 for real-time monitoring.

Table 2-2: The assigned function for the controller's six key channels

Channel	Function	Control/Monitoring
Channel 1, 2	All-red extension	Control
Channel 3, 4	Dynamic green extension	Control
Channel 7	***Congestion level monitoring***	***Monitoring***
Channel 8	***Queue length monitoring***	***Monitoring***

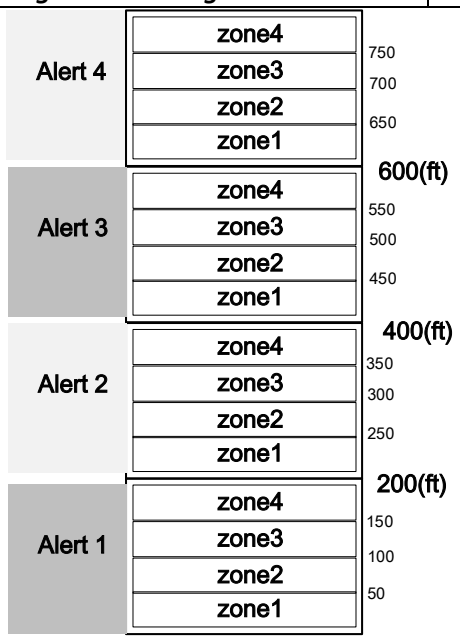

Notes:
-Vehicles that stop completely cannot be measured from the radar. Therefore, the queue formation and dissipation process can be observed, but the queue may not be observed when its length is static.
- Lanes cannot be differentiated due to the constraint of the sensor. For example, lane 1 has a queue of 100ft; lane 3 has a queue of 300ft. Then, two alerts will be concurrently shown in the above interface
- Maximum queue detected from the field is 735(ft) for WB and 750(ft) for EB

Figure 2-5: Graphical illustration of monitoring time-varying queues with the monitor.

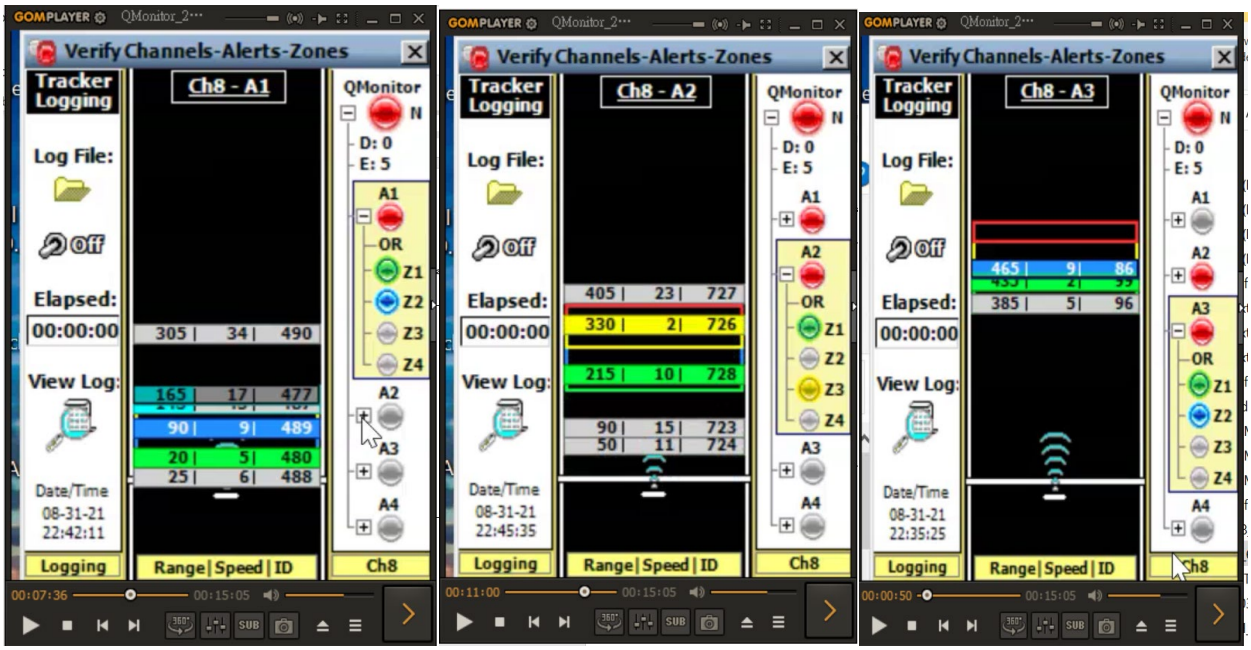

Figure 2-6: Example of detected time-dependent queue length at the MD 4 at Forestville Rd.

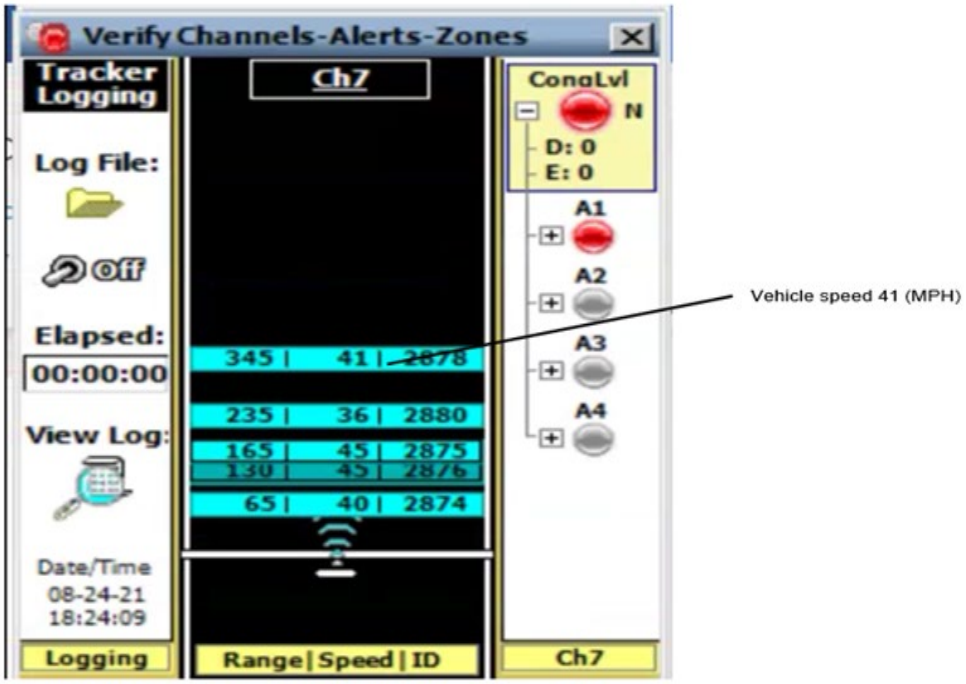

Figure 2-7: Example of displaying the detection speed by the sensor with the remote monitor.

Sensors BB and DD

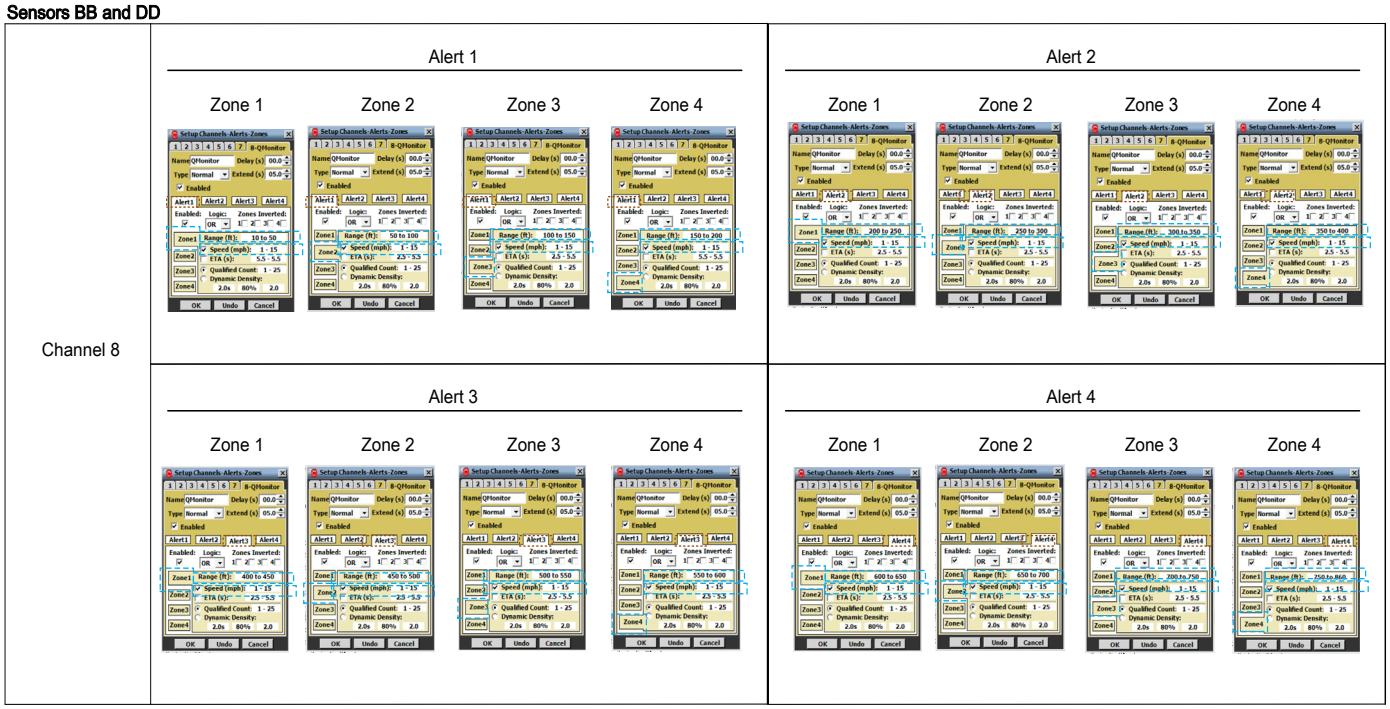

Figure 2-8: Graphical display of the queue length detection within each subzone via Channel 8 for real-time monitoring.

Chapter 3: Algorithms for Preventing Intersection Rear-end Collisions with an Optimized Dynamic Two-stage Actuated Control

3.1 Introduction of core control algorithms

As stated in the last chapter, a DARE system is designed to prevent side-angled crashes by red-light runners or drivers taking aggressive actions during the yellow phase. Since a detailed illustration of the algorithm for DARE and its field demonstration results are available elsewhere (e.g., Park et al., 2016; 2018), this chapter will focus on discussing two new control algorithms developed to prevent rear-end collisions at high-speed intersections, sharing the same hardware as DARE.

Different from the conventional design of using the "gap-out" logic to terminate the green phase for actuated signal control, this study presents two safety-based algorithms to minimize the risk of rear-end collisions during phase transition and sharing the same wide-range sensor for DARE, which can track each vehicle's speed as well as location within its detection zone of up to 228.6 meters (750ft) at the 0.1-second update interval (Wavetronix, 2016). Based on the spatial distribution of detected vehicles and the evolution of their speeds within the monitoring zone, the proposed system can execute either an enhanced gap-out control or a two-stage dynamic algorithm to terminate the green phase at the optimal time point. This minimizes the likelihood of incurring rear-end collisions between vehicles when the green phase is to be terminated or reach its maximum under an actuated signal control environment.

Algorithm 1 developed in this study is extended from the state-of-the-practice "gap out" control logic that is relatively straightforward for comprehension and implementation. Algorithm 2 is a more sophisticated control logic that can dynamically extend the green duration based on the projected speeds and locations of vehicles within the detected zone, and reduce the risk of incurring rear-end collisions if terminating the green phase at any time point over the next pre-specified time horizon. A detailed description of the core logic, parameters, and operational procedures associated with each of these two control algorithms for preventing rear-end collisions under actuated signal control is presented in the next section.

3.2 Algorithm 1: Enhanced gap-out (EGO) control with a wide-range sensor

Fig. 3-1 (a) shows the core logic of a conventional actuated control that depends on the preset critical threshold and gaps measured from a typical point-detector to execute the gap-out control strategy. Such control in practice may encounter the following two undesirable scenarios from a safety perspective:

- The speed and position of the vehicle that follows the one triggering the gap-out action by the signal are not known to the controller; and
- Multiple vehicles may be within their dilemma zones when the signal is executing the "max-out" action.

Hence, depending on the speed and distance to the intersections, vehicles within the above two scenarios may incur rear-end collisions or side-angled crashes due to red-light running.

The proposed enhanced gap-out (EGO) control is designed to prevent the approaching vehicles from encountering the above scenarios, and thus minimize the likelihood of causing any rear-end collisions during either "gap-out" or the "max-out" actions. Its core logic, as shown in Fig. 3-1 (b), is to execute the "gap-out" action only if all vehicles within the detection zone (e.g., 228.6 m from the intersection stop line) of the wide–range sensor are out of their respective dilemma zones. Since the dilemma zone for approaching vehicles varies mainly by their approaching speeds and distances to the intersection, one can implement the EGO control in practice with the following steps:

- Precompute the dilemma zone distribution for vehicles of different approaching speeds to the target intersection approach, see Fig. 3-1 (c);
- Convert the field-calibrated distribution of dilemma zones into the control variable, defined as time-to-stop-line (TSSL) and as used in the literature (Sheffi and Mahmassani, 1981; Zimmerman, 2007; Sharma et al., 2007; Hurwitz et al., 2010; Sharma et al., 2011; and Hurwitz et al., 2012);
- Compute the speed and distance to the intersection's stop line for all vehicles within the detection zone of the wide-range sensor, and then

- Execute the "gap-out" action (point B in Fig. 3-1 (b)) if the elapsed green duration has exceeded the minimum green (point A in Fig. 3-1 (b)) and all detected vehicles are out of their own dilemma zones.

Note that an alternative to replace the time-consuming off-line computation of dilemma zone distribution for vehicles of different speeds is to adopt the dilemma zone definition of "*probability of stopping of more than 10% but less than 90%*" by Parsonson et al. (1979), and calibrate these boundaries (also known as type-II dilemma zones) for vehicles to take the stop action when encountering the yellow phase.

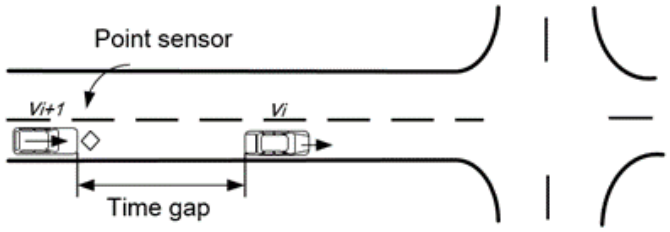

Figure 3-1(a): The state-of-the-practice logic for actuated signal control.

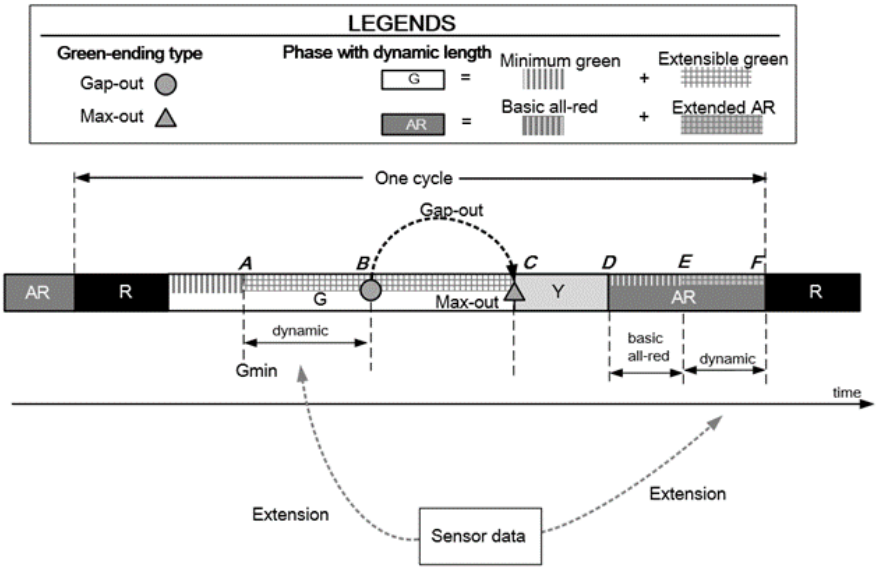

Figure 3-1(b): The algorithm for enhanced gap-out (EGO) control with a wide-range sensor.

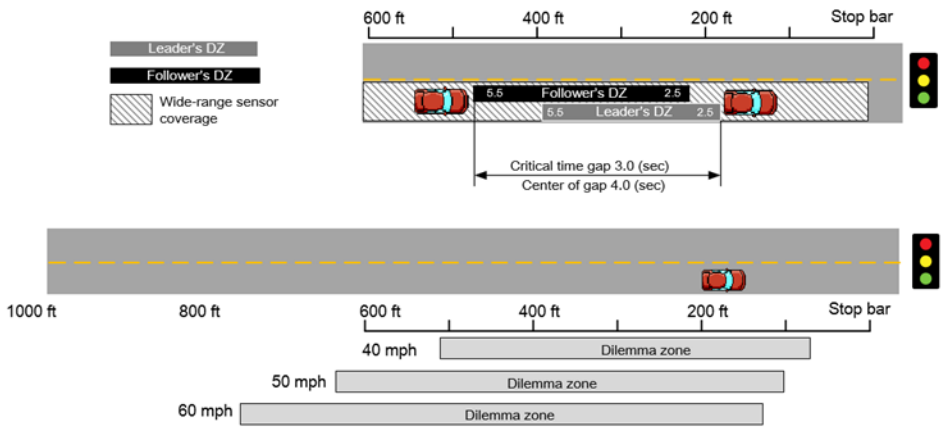

Figure 3-1(c): Graphical illustration of the algorithm for re-estimating the distribution of dilemma zones based on the updated traffic information.

In brief, Algorithm 1 features the capability of using the rich temporal and spatial information of detected vehicles' evolution within the wide-range detection zone, offering significant improvement to both the operational efficiency and the collision risk under the conventional actuated control with a point-based detector, such as a single or double loop.

3.3 Algorithm 2: Dynamic two-stage control

Note that some vehicles at the intersection operated with the Algorithm 1 control may still be trapped in their dilemma zones when the green phase reaches its preset maximum (i.e., max-out). For those choosing to take the stop action during the max-out scenario, it is still highly likely that they may incur a rear-end collision with aggressively following vehicles. Hence, this study has further proposed Algorithm 2 to minimize the likelihood of having such rear-end collisions, using the same hardware as Algorithm 1 and DARE.

The core logic of Algorithm 2, as shown in Fig. 3-2, is to divide the green-termination control into the following two stages:

- **1st stage**: Covering the duration from the minimum green to time point M (a parameter to be calibrated) during which the signal control shall operate the gap-out action with the same logic as for Algorithm 1; and

- **2nd stage**: Including the green duration from the end of the 1st stage to the maximum green time (i.e., from M to Q in Fig. 3-2) during which the signal controller shall select the dynamic "time point" (i.e., time point N in Fig. 3-2) for green termination with Algorithm 2, to minimize the likelihood of incurring any rear-end collision due to the phase transition.

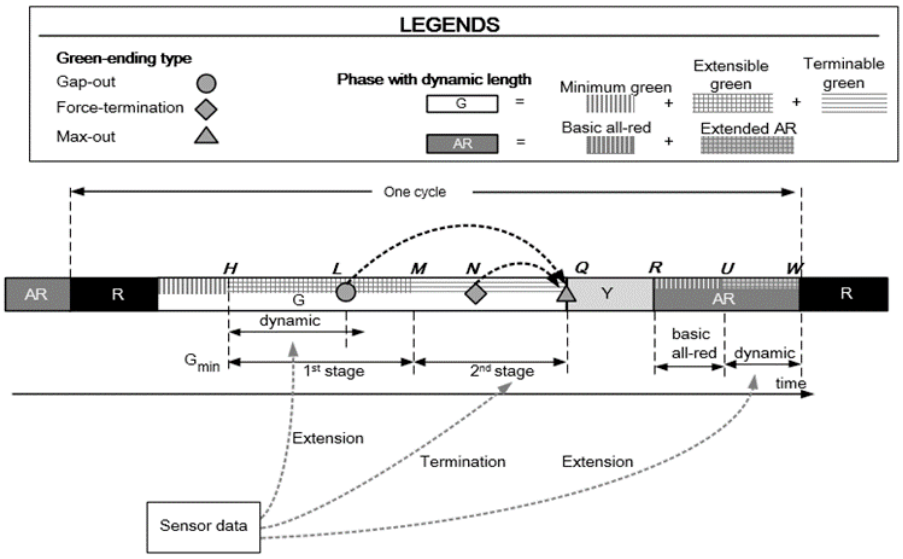

Figure 3-2: A two-stage intelligent control for actuated signal with a wide-range sensor.

Conceivably, by dividing the green duration for the stage 2 control into several sliced time increments, one can then apply various risk analysis methods to estimate the optimal sliced time point, during which the probability of having a rear-end collision between each pair of successive vehicles within the detection zone is projected to be the lowest during the entire stage-2 green period. Fig. 3-3 illustrates one such method proposed in this study to project the time-varying risk of incurring rear-end collisions between each pair of successive vehicles within the detection zone during the stage-2 green duration, where the sliced time point with the lowest total risk shall be the time for the controller to terminate the green phase before reaching "max-out".

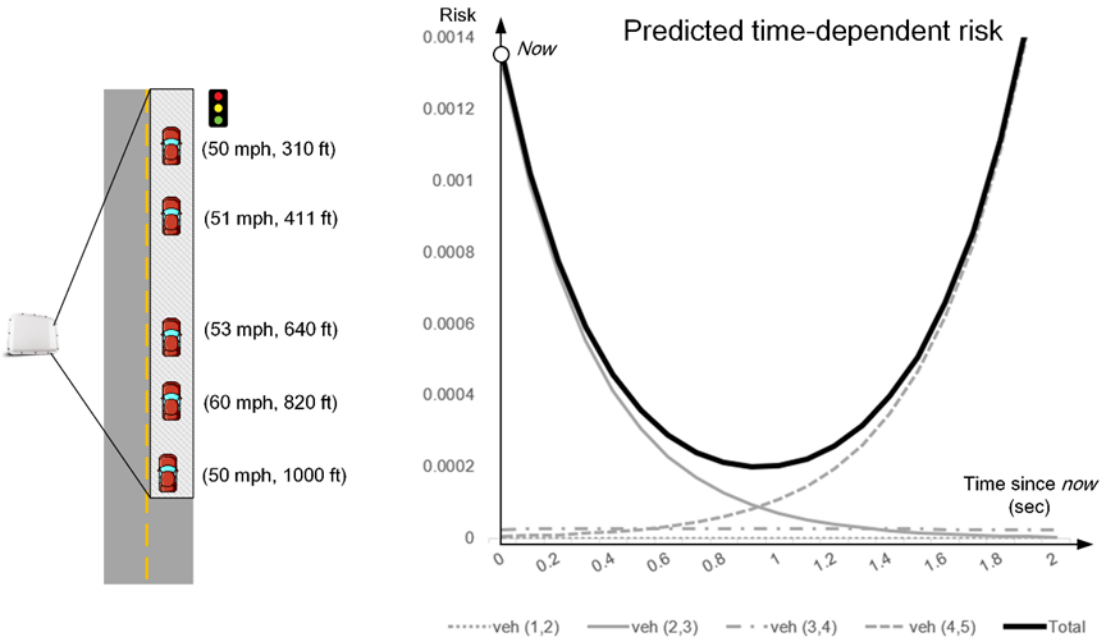

Notes:
1. Gray lines are risk accounting for a pair of leading-following vehicles whereas black line represents the overall risk.
2. Parameters βo=-0.952, βv=0.400, and βx=-0.0408 are applied to determine stop-or-pass decisions.

Figure 3-3: The algorithm for projecting the risk of rear-end collisions over time.

Fig. 3-4 shows the operational flowchart of the proposed two-stage actuated signal control process, including the interrelations between its key components and control parameters. The equations for risk prediction will be discussed in the next section.

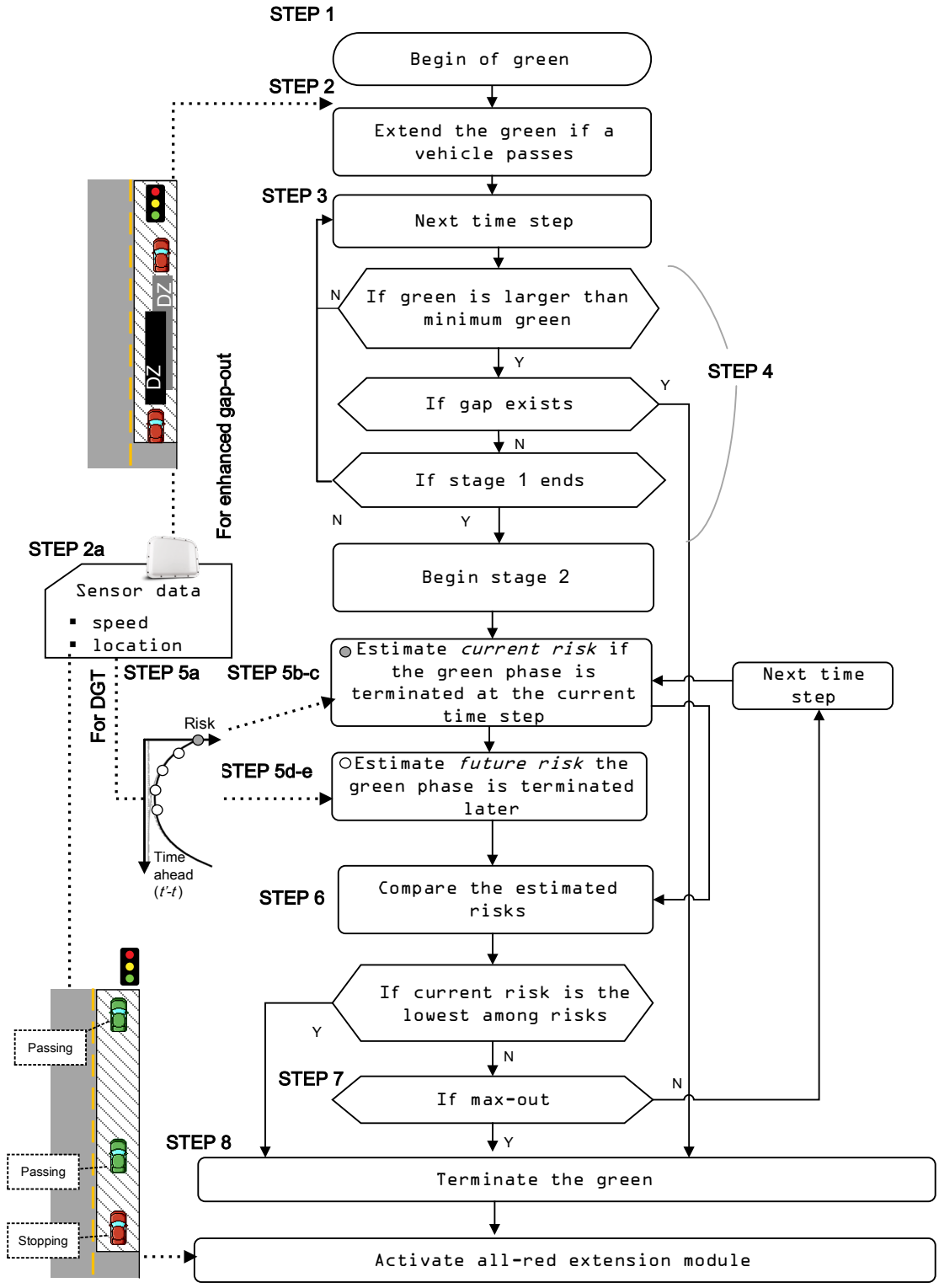

Figure 3-4: The operational flowchart for the two-stage dynamic actuated control.

Note that an alternative to circumventing the task of risk projection is to compare the number of vehicles trapped in their own dilemma zones based on their current and estimated speeds and times to the intersection at each sliced interval during the stage-2 green duration. The effectiveness of such an alternative, however, highly depends on the precision of the off-line calibrated distribution of dynamic dilemma zones for all vehicles approaching the target intersection at different speeds.

In brief, with all identified control parameters, one can convert the Algorithm 2 control with a sequence of execution steps, shown as follows:

STEP 1: Initialize timers for actuated control in green phase

1a) $t \leftarrow 0$

1b) $\tau_G \leftarrow 0.0$ *for the gap-out timer*

STEP 2: Retrieve the data from wide-range sensors and extend the green if any vehicle is in DZ.

2a) Data from wide-range sensors with location x_i *and speed* v_i *for each vehicle*

2b) Calculate TSSL (e_i*) for each vehicle by* $e_i = x_i/v_i$

2c) IF any vehicle i *satisfies* $e_L \leq e_i \leq e_U$*:*

THEN $\tau_G \leftarrow$ *VEH_EXT*

This step resets the gap-out timer with unit extension VEH_EXT if any vehicles satisfying in DZ.

STEP 3: Update all the timers

$t \leftarrow t + 0.1$

$\tau_G \leftarrow \tau_G - 0.1$

STEP 4: Termination criterion for the gap-out module

4a) IF $t \geq g_m$ *and* $\tau_G = 0$

THEN go to step 8 (gap-out immediately if dynamic gap is detected)

4b) IF $t = g_1$*:*

THEN Go to step 5 (end of stage 1, steps into terminable green)

ELSE Repeat Step 2 to 4.

STEP 5: Retrieve data from wide-range sensors and compute the risks for current and future times so comparisons can be made in the next step.

5a) Data from wide-range sensors with location x_i *and speed* v_i *for each vehicle*

5b) Estimate current probability of stopping of each vehicle by eq (3)

5c) Predict current risks by eq (2)

5d) FOR future timings t' $\in \{t + \Delta s, t + 2 \cdot \Delta s, t + 3 \cdot \Delta s \ldots t + T_L\}$*:*

Estimate projected probability of stopping of each vehicle by eq (4)

5e) Predict future risks $R_{t'}$ *by eq (2) for each t'*

STEP 6: Compares the future risks to current risks.

FOR each t'*:*

IF $R_{t'} < R_t$*: (future lower risk is a veto to terminate at current moment)*

THEN go to step 7 (not terminating)

Go to step 8 (current risk is minimal, green termination. Only when all future risks no smaller than current value can it justify terminating green immediately is the safest.)

STEP 7: Update the timer and check if maximum green is reached

7a) $t \leftarrow t + 0.1$

7b) IF $t = g_M$

THEN go to step 8 (max-out)

ELSE repeat Step 5 and 6.

STEP 8: Change from green to yellow phase. Activate dynamic all-red extension module.

3.4 System implementation

To implement the above functions by Algorithm 2 on the day-to-day intersection control practice, one shall conceivably have to perform the following two calibration tasks from the field data: the model parameters for assessing the risk of rear-end collisions, and the key parameters embedded in both control algorithms.

Assessment of rear-end collision risk

Notably, a reliable model for predicting the likelihood of incurring rear-end collisions between vehicles in the detection zone during the stage-2 green duration is the key to the success of the Algorithm 2 actuated control. To develop such a model, this study first defines the risk of incurring a rear-end collision between two successive vehicles as the following joint probability:

$$r(t) = P_{i,t}^{Stop} \cdot P_{i+1,t}^{Pass} \qquad (3\text{-}1)$$

where the left-side of (Eq.3-1) denotes the joint probability for the leading vehicle (i.e., vehicle i) to take the stop decision and the following vehicle (i+1) to exercise the passing action at the projected time point t. With such a definition for collision risk, one can further formulate the total risk of incurring any rear-end collision among any pair of successive vehicles within the detection zone during the stage-2 green duration with Equation 3-2:

$$R(t) = \sum_i \underbrace{P_{i,t}^{Stop}}_{\substack{Leader's \\ stopping\ prob}} \cdot \underbrace{(1 - P_{i+1,t}^{Stop})}_{\substack{Follower's \\ passing\ prob}} \qquad (3\text{-}2)$$

Note that there are various factors that may affect the decision of drivers when facing phase transition. However, as reported by Liu et al. (2011), vehicle speed and distance to the intersection are the two most critical factors that may have the most impact on a driver's decision under such scenarios, and are measurable from field observations at the desirable level of accuracy. Using their suggested empirical equation, one can estimate the probability of a vehicle, detected at time point t and approaching the intersection at the speed and distance of v_i^t and x_i^t, to take the stop decision as follows:

$$P_{i,t}^{Stop} = \frac{1}{1+exp\,(\beta_0+\beta_v v_i^t+\beta_x x_i^t)} \qquad (3\text{-}3)$$

where, v_i^t and x_i^t are the speed and location of vehicle i at time t and β_0, β_v, and β_x are parameters in a binary choice decision.

Therefore, with the assumption that the detected vehicles will move at the same traveling speeds, one can compute the predicted probability ($\hat{P}_{i,t'}^{\mathrm{Stop}}$) for vehicle i to take the stop action at the projected time point ($t' > t$) within the stage-2's remaining green duration as follows:

$$\hat{P}_{i,t'}^{Stop} = \frac{1}{1+exp\,(\beta_0+\beta_v v_i^t+\beta_x x_i^t-\beta_x v_i^t(t'-t))} \qquad (3\text{-}4)$$

Key parameters to be calibrated from field data

Control Strategy 1: To apply the enhanced gap-out control, one shall calibrate the boundaries of the dilemma zone (e_L, e_U), which shall be sufficiently wide to cover those vehicles approaching the target intersection at different speeds.

$$\boldsymbol{\theta}^1 = [e_L, e_U] \qquad (3\text{-}5)$$

Control Strategy 2: For implementing the dynamic two-stage control, it is essential to calibrate the following additional parameters from the field data:

$$\boldsymbol{\theta}^2 = [e_L, e_U, T, T_L, \Delta s, \beta_0, \beta_v, \beta_x] \qquad (3\text{-}6)$$

Where:

Stage-1 control interval (T): As shown in **Fig. 3-5**, there exists an optimal duration to be calibrated from the field data for stage-2 control (i.e., between point M and Q in Fig. 3-2) that can balance the efficiency of stage-1 "gap-out" operations with the risk of reaching the "max-out" to terminate the green phase. Conceivably, a longer interval for stage-1 will reduce the number of decision time points available for stage-2 to terminate the green phase at the lowest rear-end collision risk, but it is more likely to proceed with the phase transition efficiently with the algorithm-1's "gap-out" operations.

Unit interval for comparison and update (Δs): This is the length of each sliced time increment within the stage-2 green duration, mainly serving as the update interval to reflect the state of detected vehicles within the detection zone. Its optimal value, varying with the car-following behaviors and the precision of the sensors, can be identified from the simulation-based calibration.

Look-ahead horizon (T_L) within the stage-2 period: It is the key parameter for determining the number of future unit time intervals to be included in projection and comparison of their total rear-end collision risks.

Behavioral parameters ($\beta_0, \beta_v, \beta_x$) used in Eq.(3-4) to reflect the decision of drivers during the phase transition at various speeds and different distances to the target intersection. A detailed discussion of their calibration is available elsewhere (Park et al., 2016).

To allow the proposed system to operate at the most effective and reliable level, this study has adopted the following two-phase calibration with respect to key system parameters:

Phase-1 calibration: Phase-1 calibration is mainly focused on replicating the traffic conditions and driver behaviors with a microscopic traffic simulator, especially with respect to the distribution of time-varying volumes, approaching vehicle speeds, acceleration/deceleration rates, and their responses during the yellow phase under various decision scenarios. A detailed discussion of the step-1 calibration can be found in the work by Park *et al.* (2016).

Phase-2 calibration: The primary task during this phase is to apply an efficient search algorithm to identify the set of optimal parameters (shown in Eqs. (5) and (6)) that can result in the lowest number of rear-end collisions from a comprehensive set of intersection traffic scenarios generated from the traffic simulator calibrated in Phase-1. More specifically, the objective function of the phase-2 parameter calibration, which aims to minimize the projected rear-end crashes with the proposed algorithms, can be stated as follows:

$$\boldsymbol{\theta}^* = \underset{\boldsymbol{\theta}}{arg\ min}\, K \qquad (3\text{-}7)$$

where $\boldsymbol{\theta}$ is the set of parameters and K is the annual rear-end collisions at the target intersection under the given traffic conditions, driver behavioral patterns, and the adopted parameters for either Algorithm-1 or Algorithm-2 control. Note that the intersection traffic collisions under all existing traffic simulators can only be approximated with the surrogate variable; that is, the number of traffic conflicts between various traffic movements.

By adopting the well-accepted empirical relationship from Federal Highway Administration's surrogate safety assessment model (SSAM) (Gettman and Head, 2003), one can convert the hourly number of conflicts to an annual number of collisions:

$$K = K_0 \cdot Y^{1.419} \qquad (3\text{-}8)$$

where Y is the hourly conflict and K_0 is a constant.

Due to monotonicity of (8), equation (7) can be equivalently formulated as:

$$\boldsymbol{\theta}^* = \underset{\boldsymbol{\theta}}{arg\ min}\, Y \qquad (3\text{-}9)$$

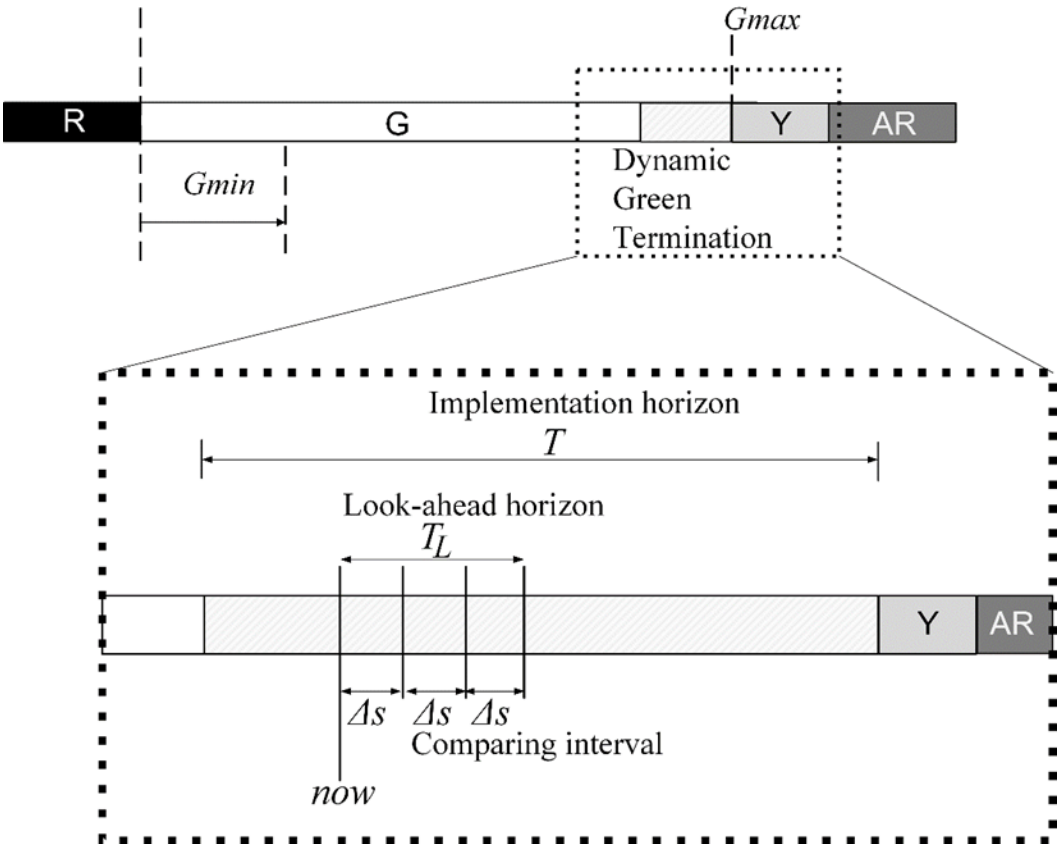

Figure 3-5: Parameters must be considered for comparing the risk of collisions.

Figure 3-6 shows the flowchart of such a search process with our selected search algorithm, SPSA (see, e.g., Spall (1992); Chau and Fu (2015); Bhatnagar (2012)) and its interactive relations with the calibrated traffic simulator. Its primary logic of the search process can be summarized as follows:

- **Initialize** system parameters within feasible range and a random seed (which will vary in each iteration)
- **Generate random perturbations** from Bernoulli distribution for each parameter so the gradient to be estimated later has the expected value of the true gradient.
- **Evaluate safety performances** of the two perturbed points from VISSIM and open-source SSAM (NGSIM 2017). The random seeds used at these two points are based on a variance-

reduction technique (VRT, see Law and Kelton, 2000), a commonly used method for calibrating the gradient under a noisy stochastic condition.

- **Proceed to the improved solution** directed by approximate gradient obtained from performances of the perturbed points.
- **Check the termination criterion** and stop if fulfilled; otherwise, prepare for the next iteration by updating the iteration index and the random seed.

Note that although there are various search algorithms available in the literature for currently identifying a set of optimum parameters, this study has adopted SPSA for optimization of all key parameters for both control algorithms due to its properties of efficiency and reliability.

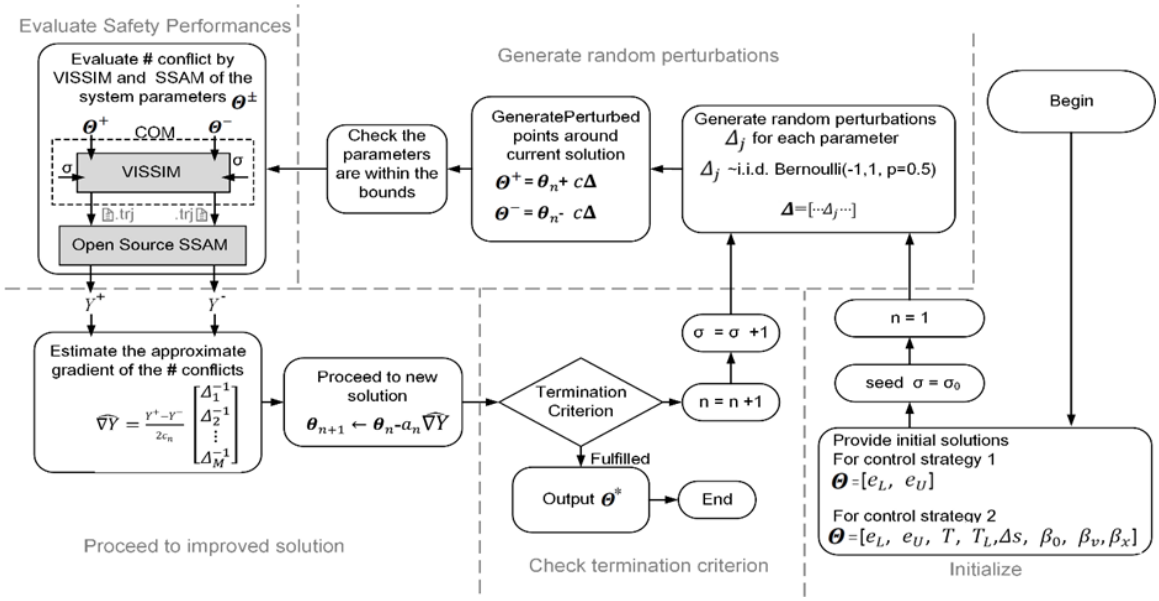

Figure 3-6: The search algorithm - SPSA for obtaining the set of optimal system parameters.

3.5 Conclusions

To minimize the likelihood of having rear-end collisions at signalized intersections, this study presents two algorithms for use with an actuated signal controller and the wide-ranger sensor, deployed for dynamic all-red extension. The first algorithm features its replacement of

conventional "gap-out" control with vehicles detected in a field-calibrated dilemma zone and executes a phase transition only if no vehicle is within the detected zone.

To further assure of no rear-end collisions during either the defaulted green "max-out" or extended "max-out", this study has further proposed a dynamic two-stage control algorithm that can optimally divide the duration between the minimum and maximum greens into two stages, where the signal within stage-1 duration will operate the first algorithm for green termination to ensure its efficiency, but shall execute the phase transition within stage-2 only at the time point projected to have the least likelihood of incurring rear-end collisions between any pairs of leading-following vehicles within the sensor's monitoring zone. Since the effectiveness of the algorithms depends on the accuracy and reliability of their key parameters, the study has detailed their operational logic and the procedures for system calibration with field data, traffic simulators, and optimal searching heuristics.

Chapter 4: Pre-deployment Analyses for candidate intersections

4.1 Introduction

This chapter presents the results of pre-deployment assessment at three candidate intersections for deploying the developed integrated intelligent intersection control system (III-CS) for improving traffic safety. The analysis for assessing the potential effectiveness of the deployment include the following tasks:

- Collecting key traffic flow characteristics associated with intersection safety such as the posted speed, spatial distribution of dilemma zones, and traffic volumes during peak and off-peak periods (see Table 4-1);
- Documenting the geographical features of the three candidate sites (see Figure 4-1), including the geometric features, limitations for deployment, and traffic patterns of the driving populations;
- Analyzing the traffic safety records and potential locations for installing traffic sensors for monitoring traffic evolution within the dilemma zones; and
- Surveying the speed distribution of vehicles approaching the candidate intersection during the green and the yellow phases within and beyond the sensor's monitoring zone.

Upon completing of the above tasks, the pre-deployment assessment will focus on estimating the risk of having rear-end collisions and angle crashes among the current driving populations, using simulation analysis with its key parameters calibrated from the target intersection's field data. The risk level revealed from the simulator that can replicate the candidate intersection's current traffic patterns and driving behaviors will serve as the basis for assessing the potential effectiveness and resulting benefits of deploying the III-CS developed in this project.

A brief review of the results from each of the above tasks is presented in the following sections.

Table 4-1: Summary of key traffic flow characteristics at three selected intersections

Site	MD 4 @ Forestville Rd.	US 301 @ Billingsley Rd.	US 301 @ Governor Bridge Rd./Harbour Way
Number of through lanes per direction	3(EB)/ 2 (WB)	2	3
Posted speed limit (MPH)	55	55	50
85th-percentile speed on yellow phase (MPH)	58.4	62.9	56.8
Type-II Dilemma Zone (seconds to stop line)	2.2 to 6.7	2.5 to 5.3	2.6 to 6.6

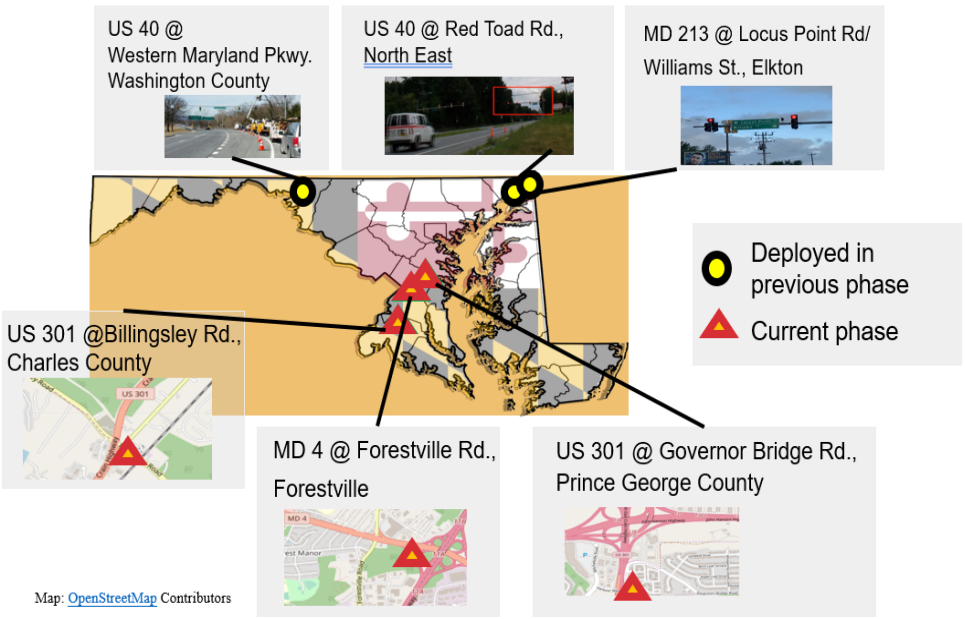

Figure 4-1: Geographical distribution of the three candidate sites for pre-deployment analysis.

4.2 Pre-deployment analyses of traffic and safety characteristics

MD 4 @ Forestville Rd.

The first candidate site (see Fig. 4-2(a)) selected for pre-deployment assessment is the intersection of MD 4 @ Forestville Rd. in Forestville, Maryland, located in Prince George's County, which has the posted speed limit of 55mph. It is on a major commuting roadway and experiences moderate congestion during peak hours. A snapshot of the peak-period congestion is shown in Figure 4-2(b). Figures 4-2(c) and 4-2(d) further display the essential information for pre-

deployment assessment, including the geometric features of the roadway segment, lane configuration, and the proposed sensor locations at the intersection of MD 4 @ Forestville Rd. The intersection's traffic volume distribution, along with its average approaching speeds during the non-congested mid-day hours, is shown in Figure 4-2(e).

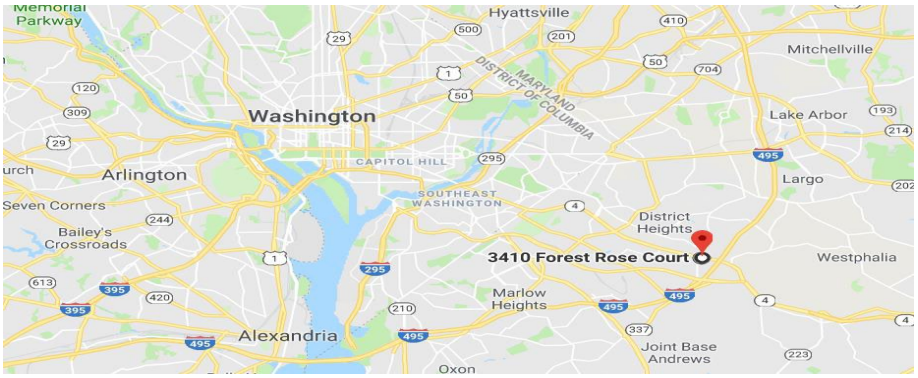

Figure 4-2(a): the location of the candidate intersection of MD 4 @ Forestville Rd.

Figure 4-2(b): A snapshot of traffic conditions viewed from Google.

Figure 4-2(c): Geometric features of the roadway to the candidate intersection of MD 4 @ Forestville Rd.

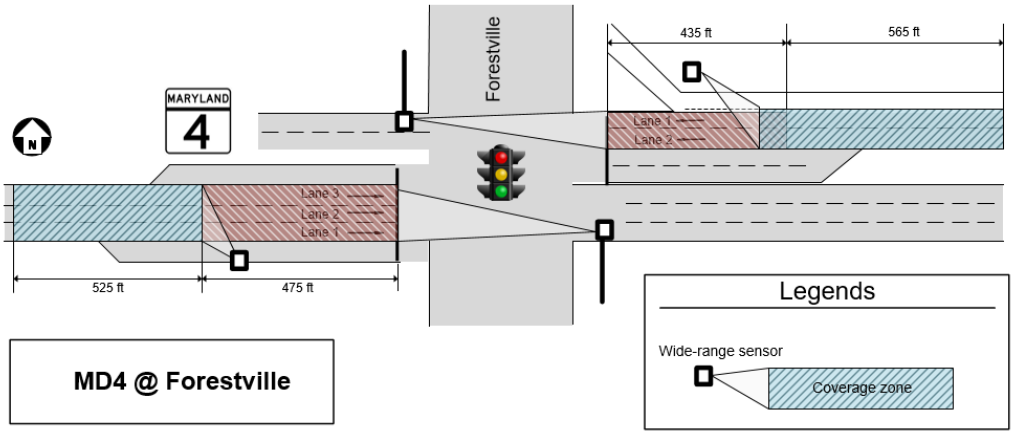

Figure 4-2(d): Geometric features, lane configuration, and sensor deployment at the intersection of MD 4 @ Forestville Rd.

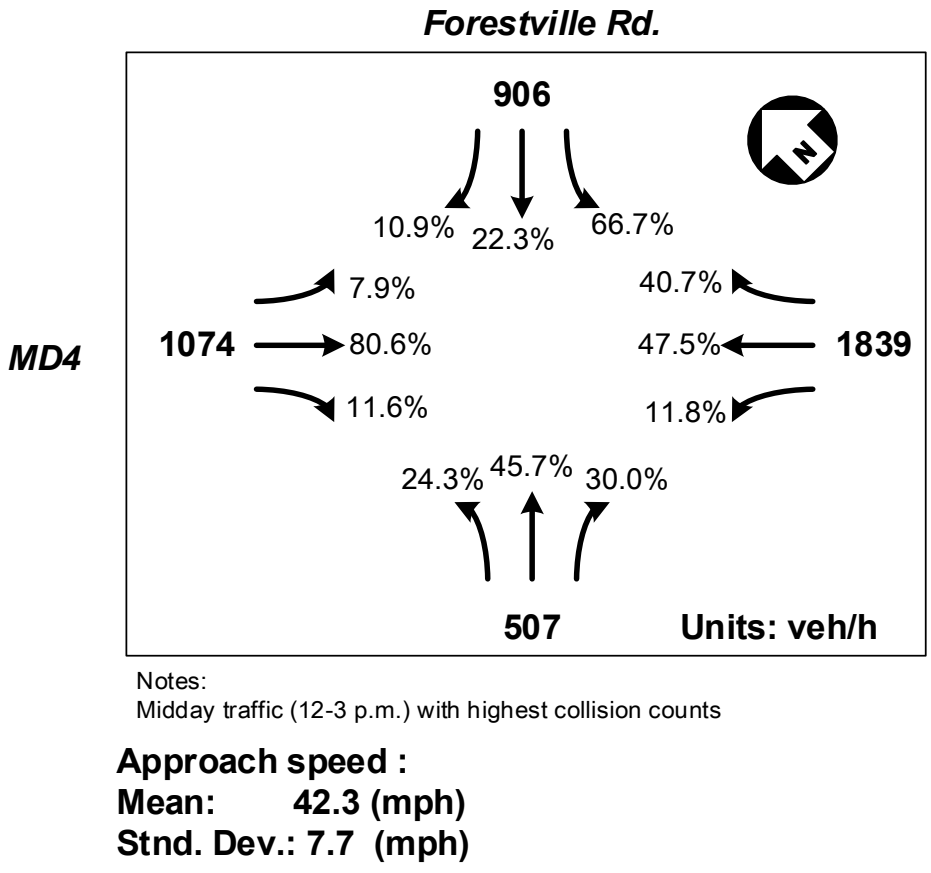

Figure 4-2(e): Traffic volume distribution and approaching speeds at the intersection of MD 4 @ Forestville Rd.

Forestville Rd. as a candidate site for deploying the III-CS is because of its high frequency of rear-end collisions. Based on the crash data from MDOT SHA (see Fig. 4.3(a)), the intersection's westbound lanes incurred 16 rear-end collisions over the past three years and resulted in seven injuries. Its eastbound lanes also suffered from a total of five rear-end collisions and five injuries during the same period.

Figure 4.3(b) illustrates the crash pattern over different times of a day, highlighting the three time periods (i.e., 8-9 am, noon-2 pm, and after 8 pm) with distinctly high average crash frequencies. Further analyses with respect to the speed profile of vehicles approaching the intersection of MD 4 @ Forestville Rd. are presented in Figures 4-4 and 4-5. As reflected in the statistical patterns, the traffic speeds are relatively uniform across all travel lanes, mostly between

40-50 mph (around 50%) at the proposed sensor-deployment location of 770 ft eastbound from the intersection.

In contrast, the speeds for the westbound lanes are relatively slower, mainly distributed between 30-40 mph at its proposed sensor location about 680ft from the intersection. Both locations, as shown in the cumulative speed statistics, have around 20% of traffic running above the posted speed limits. Conceivably, those high-speed vehicles are likely to be in their respective dilemma zones when encountering a yellow phase and thus incurring rear-end collisions.

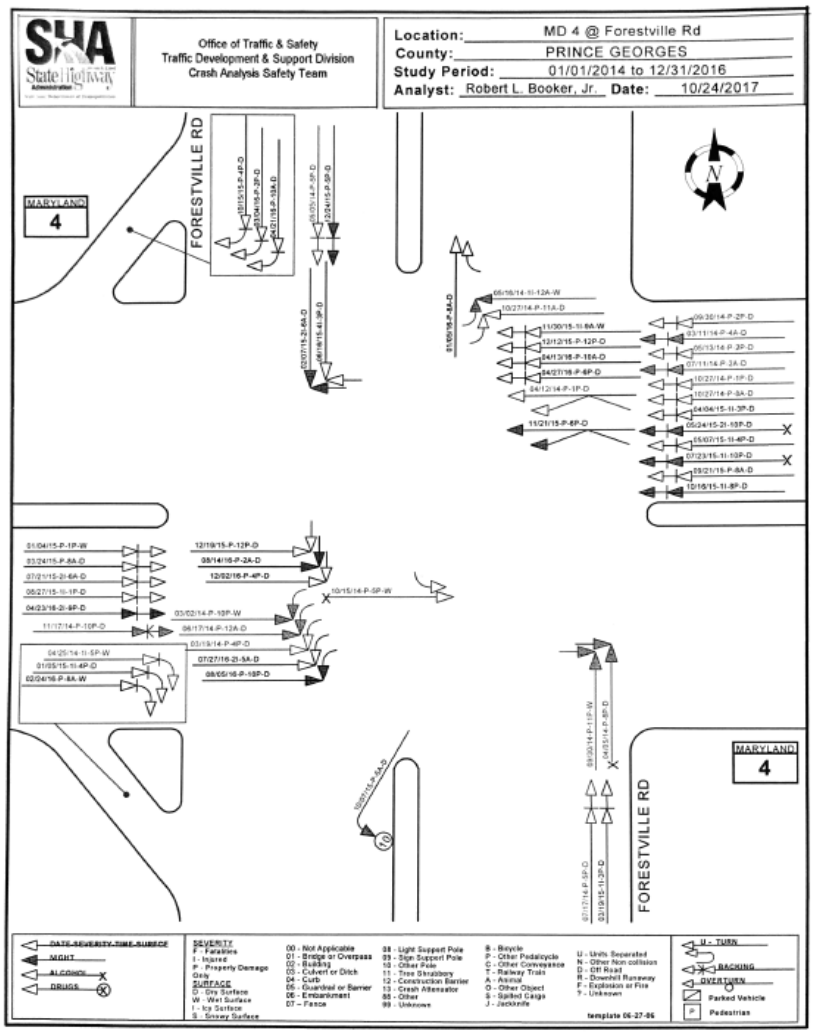

Figure 4-3(a): Collision diagram at the intersection of MD 4 @ Forestville Rd.

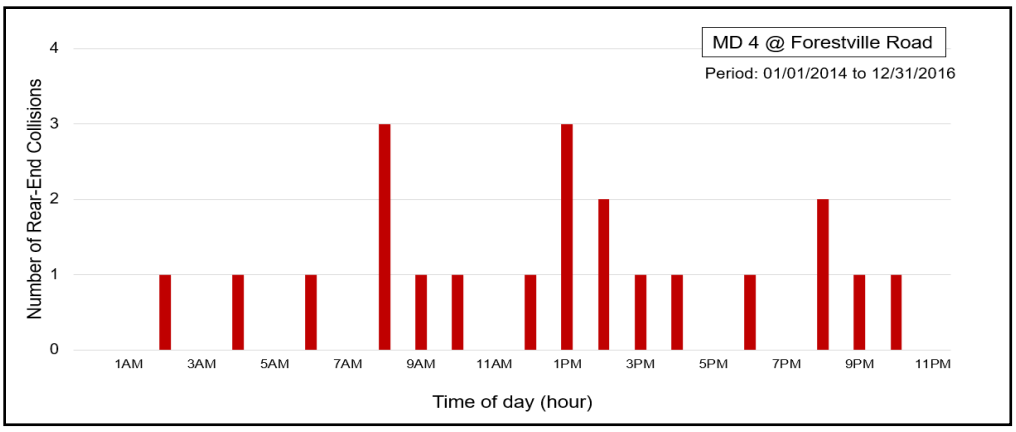

Figure 4-3(b): Number of crashes by time-of-day at the intersection of MD 4 @ Forestville Rd.

- Eastbound (770ft upstream)

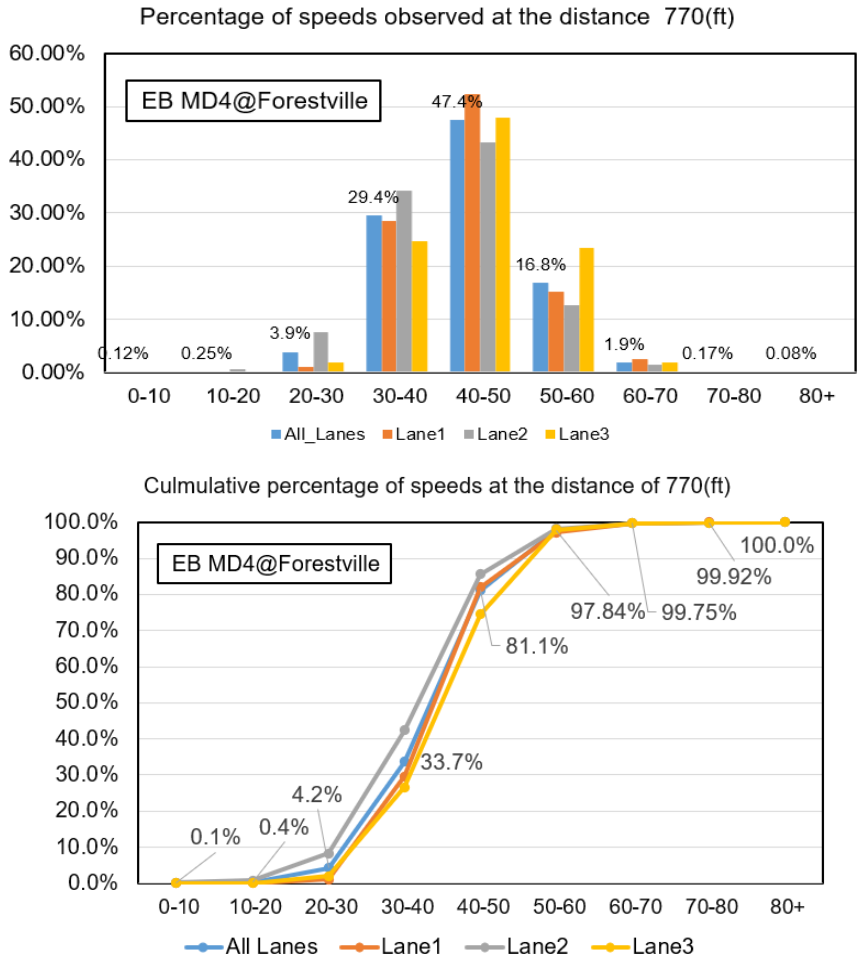

Figure 4-4: Distribution of traffic speeds in the EB of the intersection of MD 4 @ Forestville Rd.

- Westbound (680ft upstream)

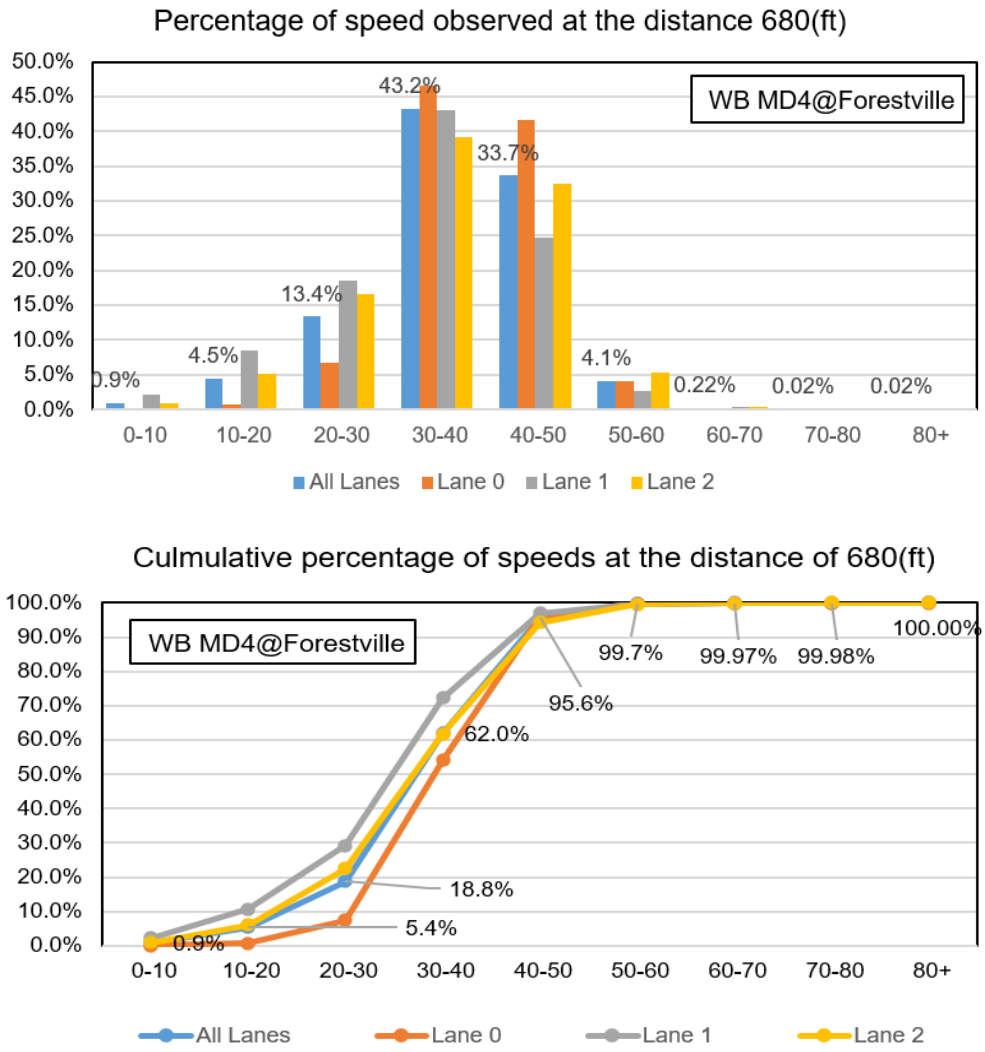

Figure 4-5: Distribution of traffic speeds in the WB of the intersection of MD 4 @ Forestville Rd.

Since a driver's improper decision when approaching the intersection during a yellow phase is the primary contributor to rear-end collisions between successive vehicles, the pre-deployment analysis of traffic characteristics should include the distribution of vehicle speeds during such critical intervals. Figure 4-6 shows the statistics of such information from the EB traffic, the one having higher approaching speeds than its opposing direction, and about 15-20% of its drivers choosing to accelerate up to 20 mph over the speed limit during the yellow phase.

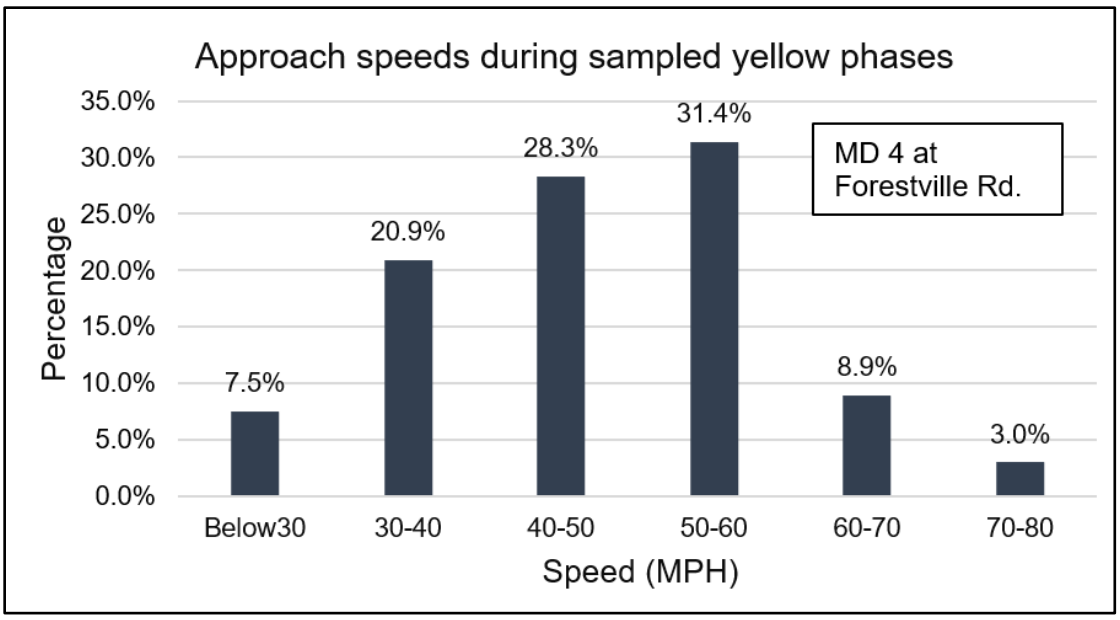

Figure 4-6: Distribution of traffic speeds during the observed yellow phases in the EB of the intersection of MD 4 @ Forestville Rd.

US 301 @ Billingsley Rd.

The intersection of US 301 @ Billingsley Rd. in White Plains, Charles County, Maryland (as shown in Figure 4-7(a)) is the second candidate site for potential deployment of the III-CS for safety improvement. Figures 4-7(b) and 4-7(c), respectively, offer a snapshot of traffic conditions in the north and south bound lanes of the candidate intersection under the posted speed limit of 55 mph. Its geometric features and lane configuration are further illustrated in Figure 4-7(d). The distribution of its traffic volume during the pre-deployment field study period is reported in Figure 4-7(e).

With respect to the safety level, this candidate site between 2014-2016 experienced a total of 10 rear-end crashes and six injuries in its north leg, and eight rear-end collisions and seven injuries in its south leg, as shown in Figure 4-8. Figure 4-9 displays the candidate intersection's distribution of rear-end crashes by time-of-day, revealing that a higher frequency of rear-end collisions occurred in both the morning peak hours and the noon time period.

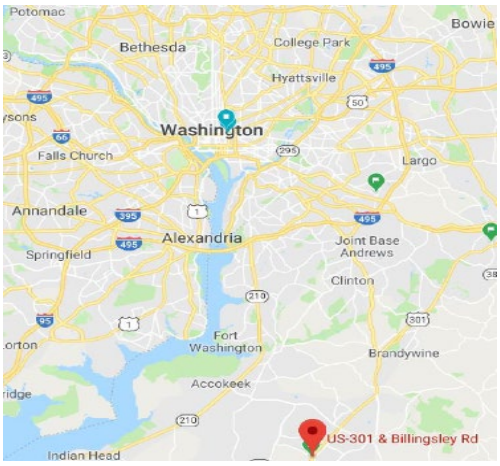

Figure 4-7(a): The location of US 301 @ Billingsley Rd., White Plains, Charles County, MD.

Figure 4-7(b): A snapshot of southbound traffic conditions at US 301 @ Billingsley Rd., White Plains, Charles County, MD.

Figure 4-7(c): A snapshot of northbound traffic conditions at US 301 @ Billingsley Rd., White Plains, Charles County, MD.

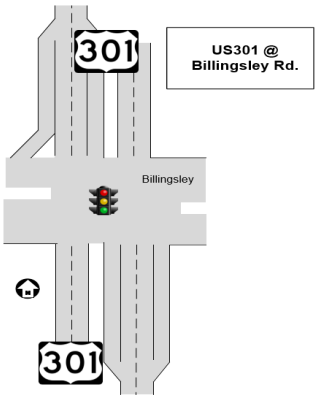

Figure 4-7(d): Geometric features and lane configuration at the intersection of US 301 @ Billingsley Rd., White Plains, Charles County, MD.

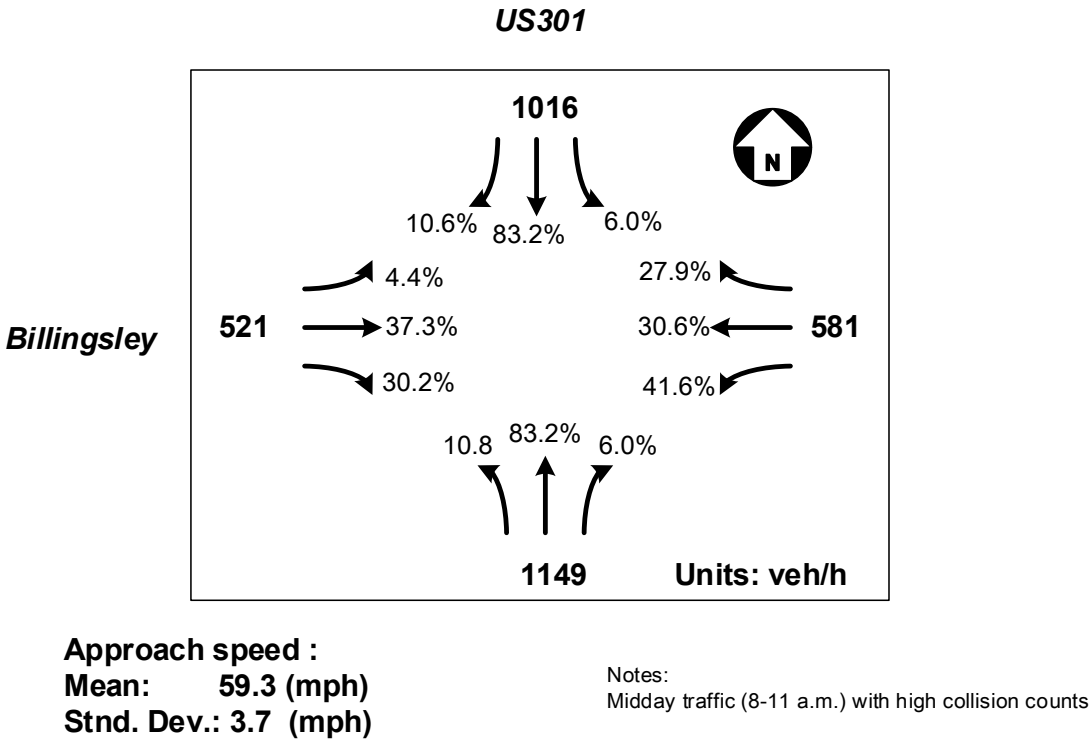

Figure 4-7(e): Distribution of traffic volumes and speed during the pre-deployment study at the intersection of US 301 @ Billingsley Rd., White Plains, Charles County, MD.

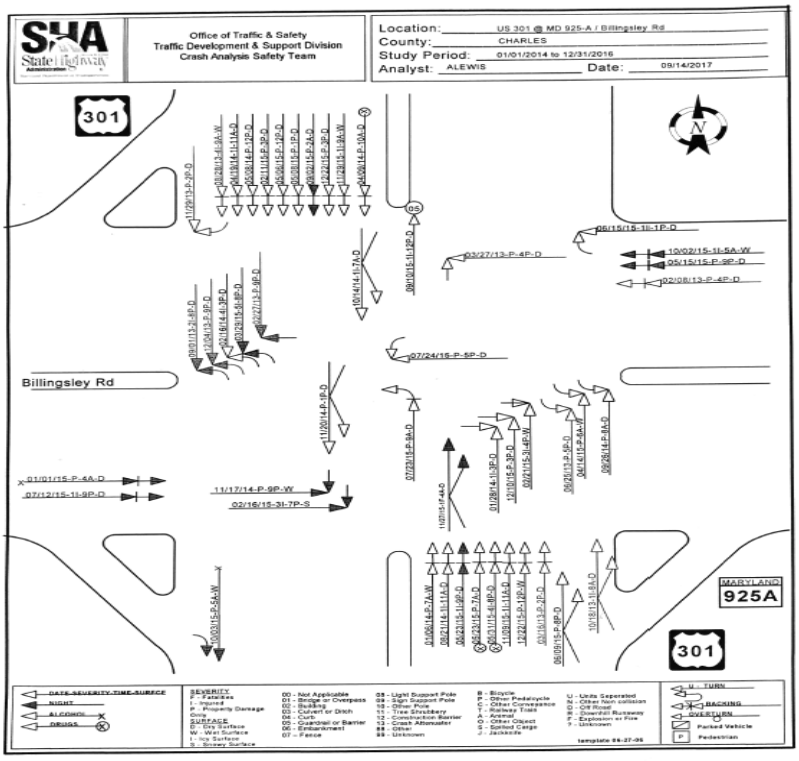

Figure 4-8: Collision diagram (2014-2016) at the intersection of US 301 @ Billingsley Rd., White Plains, Charles County, MD.

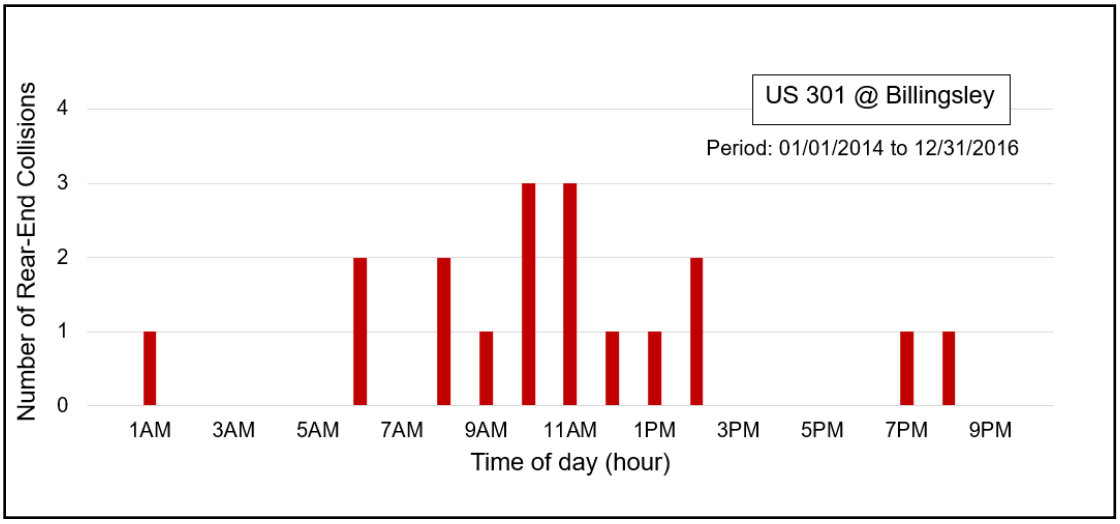

Figure 4-9: Distribution of rear-end crashes on high-speed approaches by time-of-day (US 301 at Billingsley Rd.).

As for the distribution of northbound approaching vehicles' speeds, Figure 4-10 shows that most vehicles' speeds are between 40-50 mph during non-congested periods. However, more than 25% of vehicles' approaching speeds during the yellow phases are significantly higher than the posted speed limit of 55 mph, as displayed in Figure 4-11. Most critically, it is noticeable that about 4% of drivers choose to pass through the intersection during the yellow phase at a very aggressive speed of 70-80 mph, and result in the high risk of rear-end collisions.

Note that the southbound traffic flow characteristics were not collected due to the geometric constraints for deploying roadside sensors and the safety concerns of field operators.

- Northbound speed
    - Sampling on periods without queue

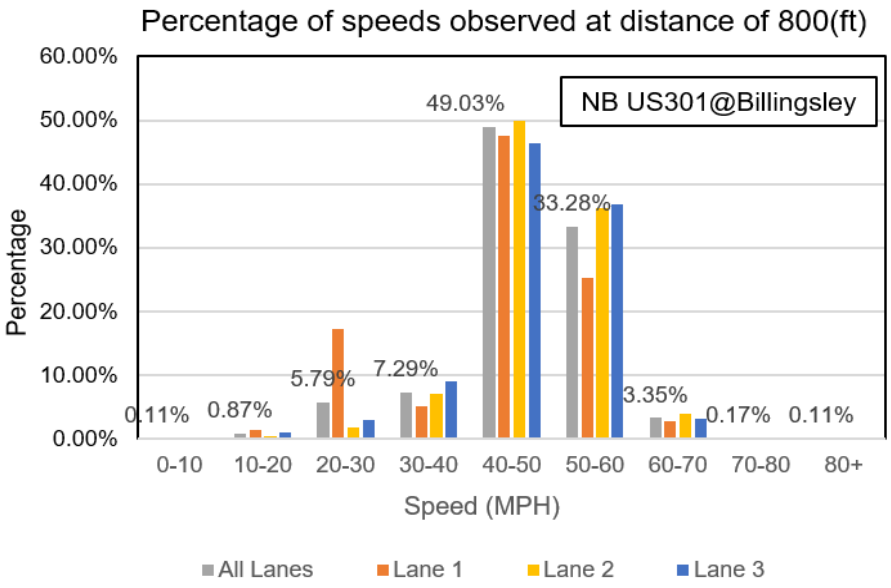

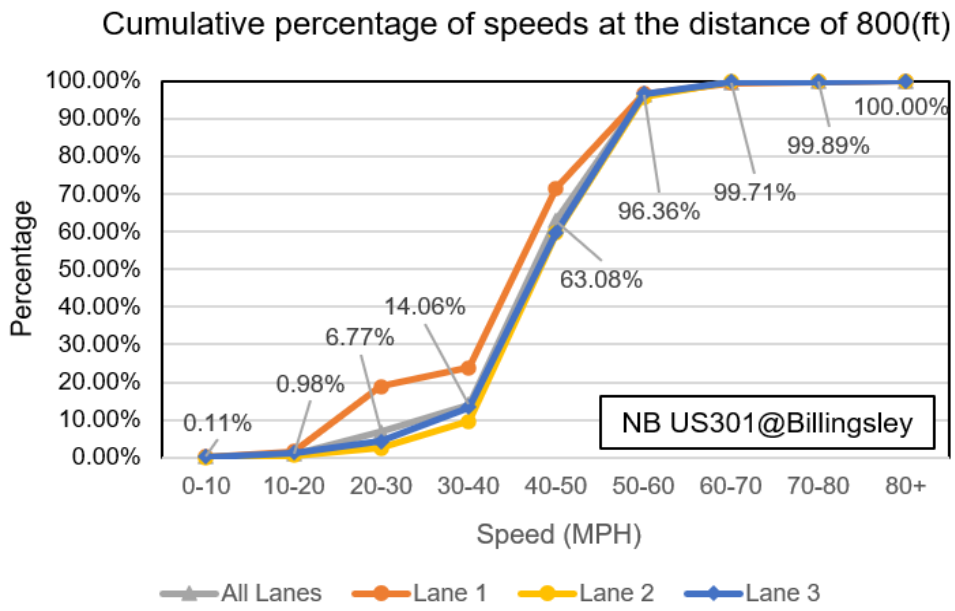

Figure 4-10: The distribution of northbound approaching vehicles' speeds.

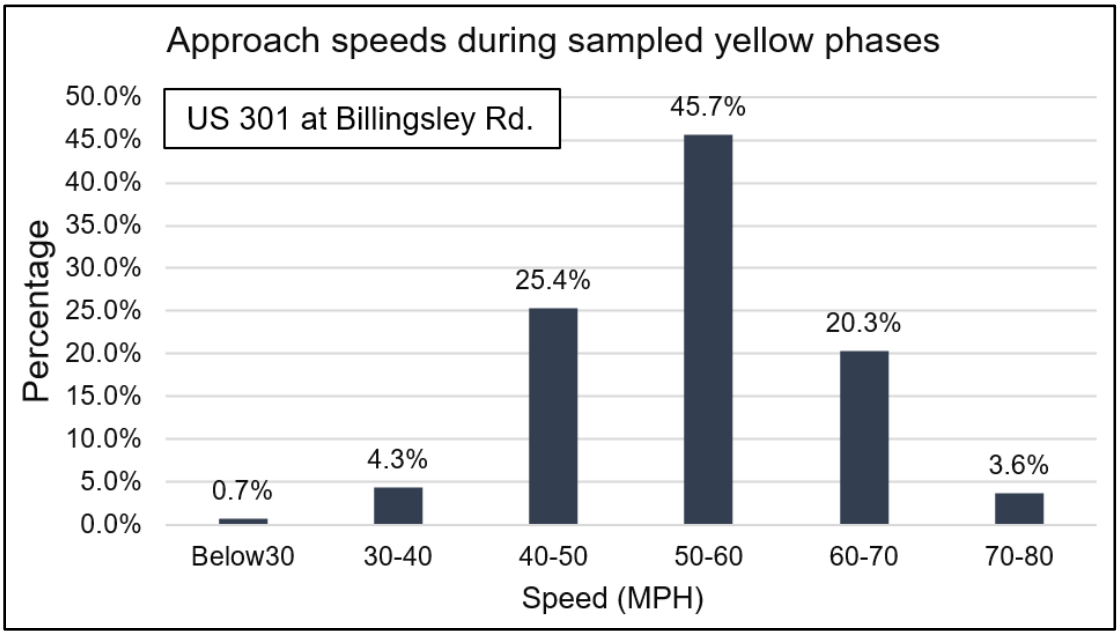

Figure 4-11: Speed distribution of approaching vehicles during yellow phases (US 301 at Billingsley Rd.).

US 301 @ Governor Bridge Rd./Harbour Way

The third candidate site for system deployment is at the intersection of US 301 @ Governor Bridge, Prince George's County, MD. Figure 4-12(a) illustrates its geographical location and the posted speed limit of 50 mph; Figures 4-12(b) and 4-12(c), respectively, show a snapshot of traffic conditions in the north and south legs of this candidate intersection. Figure 4-12(d) further displays all essential information associated with the intersection of US 301 @ Governor Bridge for the system deployment, including its geometric features, lane configuration, and locations for possible deployment of traffic sensors. Its volume distribution during the field data collection period is shown in Figure 4-12(e).

- Posted Speed Limit: 50 MPH

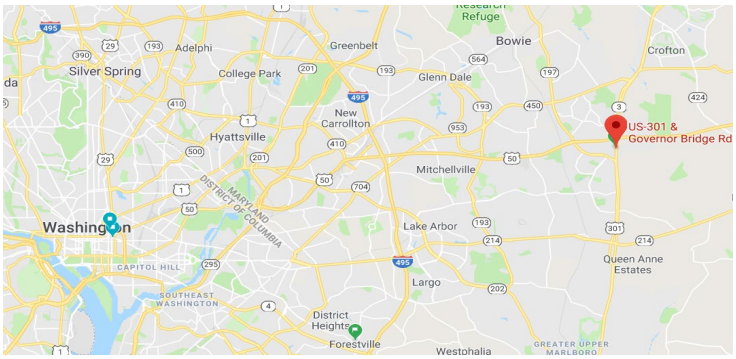

Figure 4-12(a): Geographical location of the intersection of US 301 @ Governor Bridge, Prince George's County, MD.

Figure 4-12(b): A snapshot of traffic conditions in the north leg of the intersection of US 301 @ Governor Bridge, Prince George's County, MD.

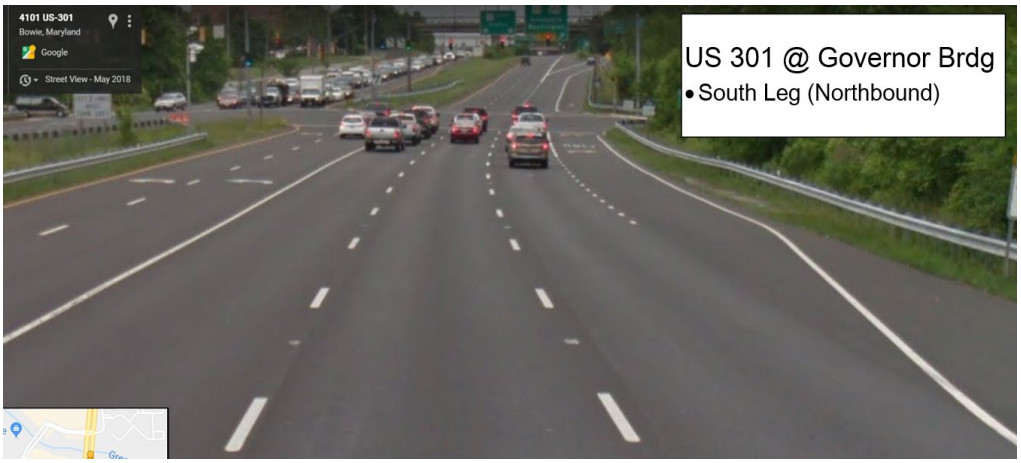

Figure 4-12(c): A snapshot of traffic conditions in the south leg of the intersection of US 301 @ Governor Bridge, Prince George's County, MD.

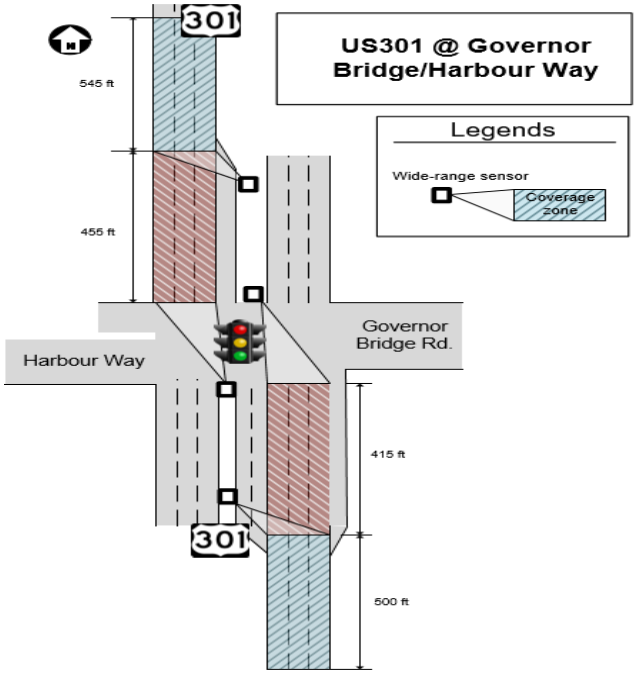

Figure 4-12(d): Geometric features, lane configuration, and locations for sensor deployment at the intersection of US 301 @ Governor Bridge.

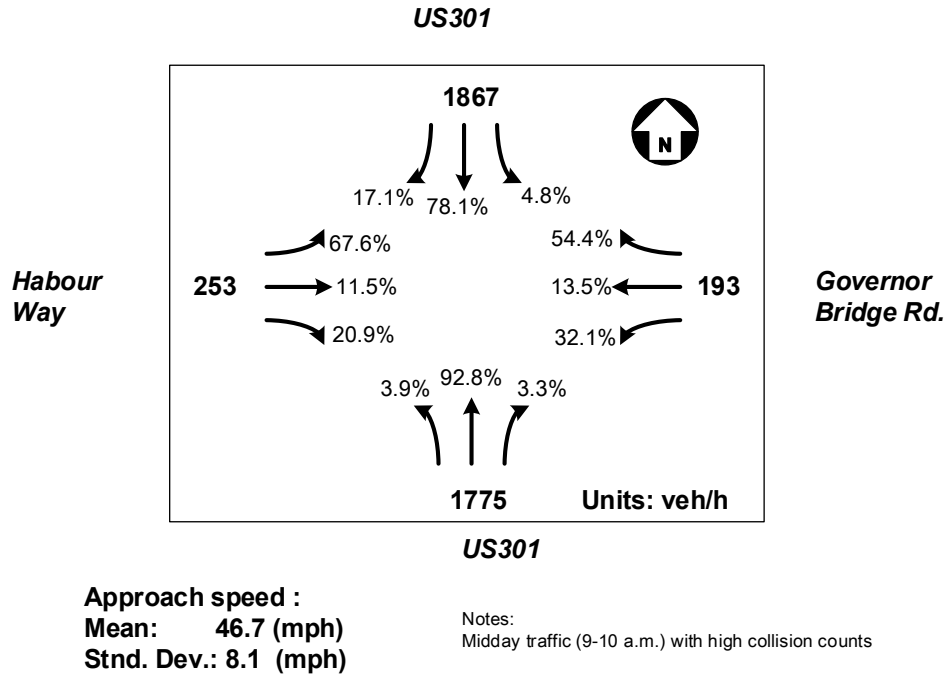

Figure 4-12(e): Distribution of traffic volumes and speeds at the intersection of US 301 @ Governor Bridge.

With respect to the safety records, this candidate intersection experienced a total of 14 rear-end collisions between 2013-2017 in its southbound lanes, resulting in l10 injuries. In contrast, its northbound traffic suffered a much more serious safety issue, exhibiting 27 rear-end collisions and 21 injuries during the same 5-year period. The distribution of crashes by time-of-day statistics further reveals that most of such accidents occurred between 8 am and 2 pm (see Figure 4-13).

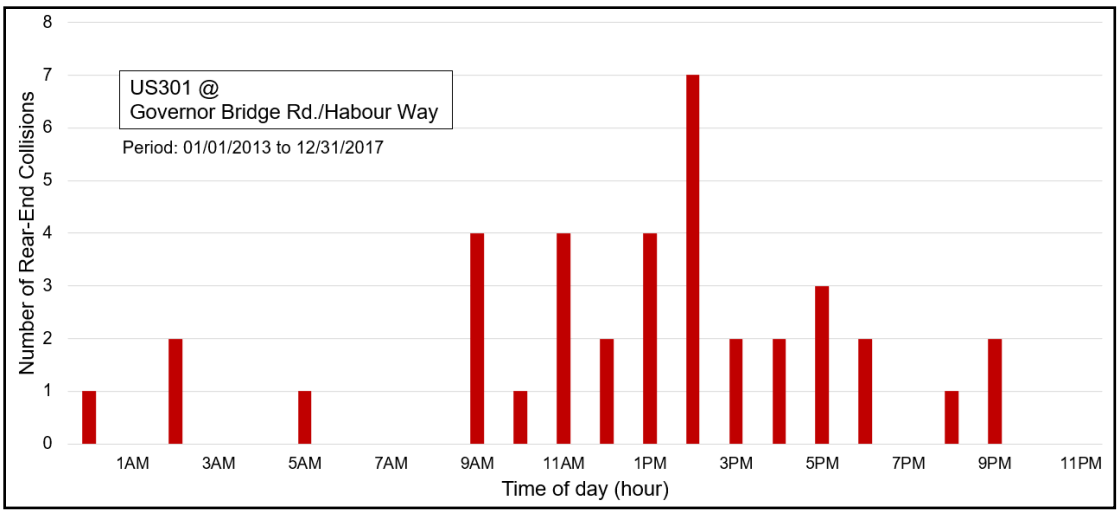

Figure 4-13: Distribution of rear-end crashes on high-speed approaches by time-of-day (US 301 at Governor Bridge Rd./Harbour Way).

With respect to the speed distribution of vehicles approaching this candidate intersection during the green phase, it is noticeable that most vehicles' speeds are between 45 to 55 mph, but some did reach the unsafe level of 70 mph, as shown in Figure 4-14. This speed distribution pattern is consistent with the speed distribution observed during the yellow phase (see Figure 4-15), where most vehicles' speeds were within the range of 45-55 mph, but about 6% of drivers passed through the intersection at speeds of 10 to 20 mph over the posted speed limit. The presence of such aggressive drivers is likely the main contributor to the intersection's high frequency of rear-end collisions.

Note that the same speed distribution data during the green and yellow phases were not collected for the northbound traffic due to the geometric constraints and the safety concern for field operators.

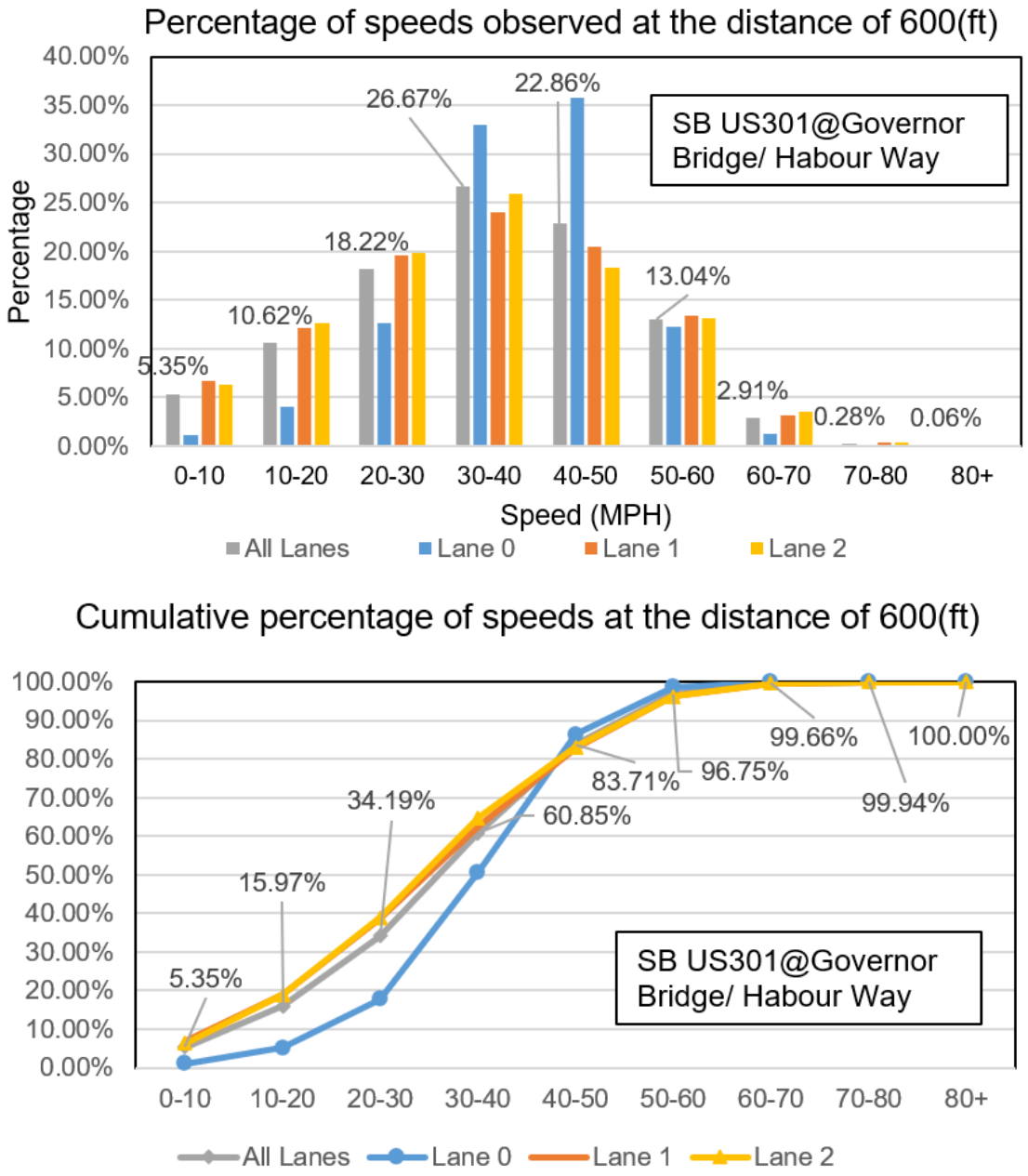

Figure 4-14: Speed distribution of approaching vehicles to the intersection of US 301 at Governor Bridge Rd./Harbour Way.

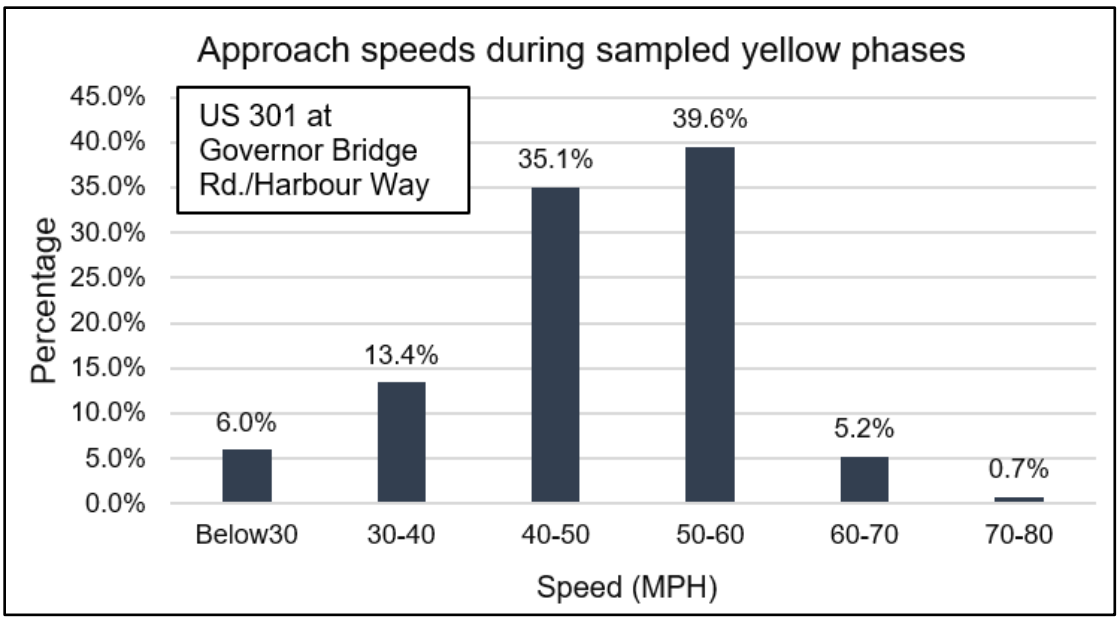

Figure 4-15: Speed distribution of vehicles approaching the intersection of US 301 at Governor Bridge Rd./Harbour Way during the yellow phase.

4.3 Traffic safety analysis for pre-deployment assessment

The purpose of pre-deployment assessment is to evaluate the effectiveness of the proposed Integrated Intelligent Intersection Control System (III-CS) for safety improvement among each candidate intersection's current driving populations. Such a system will be deployed only if the resulting probability of incurring rear-end collisions can be reduced significantly. Since the proposed system's effectiveness depends highly on the response pattern of the target driving populations during the yellow phase, one can employ a microscopic traffic simulation model with field calibrated behavioral parameters to replicate the decision scenarios encountered by drivers, and then analyze their resulting risk level—i.e., if they become trapped in the dilemma zone.

The entire pre-deployment analysis consists of the following primary steps:

- Calibration of a driver's response of "stop" or "pass" during the yellow phase with a state-of-the-art binary discrete choice behavioral model;
- Compute the spatial distribution of dilemma zones for each candidate intersection's driving populations, based on the speed distribution data collected at the proposed sensor location and different distances to the intersection stop line;

- Replicate the candidate intersection's traffic conditions and the behaviors of its driving populations with VISSIM, a microscopic traffic simulation model;
- Mathematically represent the proposed system's control algorithms and program it along with the proposed system's sensor and key decision functions to work with the calibrated traffic simulator for each candidate intersection;
- Conduct extensive simulation experiments to replicate the interactions between the proposed system and the simulated driving populations during the yellow phase at each candidate intersection; and
- Compare the measures of effectiveness for reducing collision risk with and without the proposed system at each candidate intersection.

Some primary results from each of the above steps for such pre-deployment assessment are summarized below:

Driver response models during the yellow phase

- Logit model 1 (Eq. 4-1) – for estimating the probability of a driver to take a "pass" decision when encountering the yellow phase at the given distance and speed; where v denotes the vehicle speed (ft/s), and x reflects the distance to stop bar (ft).

$$P\{pass\} = \frac{1}{1+exp\{-(\beta_0+\beta_1 v+\beta_2 x)\}} \quad (4\text{-}1)$$

- Logit model 2 (Eq. 4-2): for estimating the probability of a driver to take a "pass" decision when encountering the yellow phase, based on his/her estimated time to the intersection stop line; where E is the estimated time to stop bar (= v/x).

$$P\{pass\} = \frac{1}{1+exp\{-(\beta_0+\beta_E E)\}} \quad (4\text{-}2)$$

The performance of these two models has been evaluated with extensive simulation experiments under the field-collected driving populations and traffic conditions. Based on the assessment results and convenience for applications, this study has selected Logit model 2 for the

ensuing analysis of the proposed system's estimated effectiveness if it is properly deployed at each candidate intersection. Table 4-2 lists the two parameters of Logit model 2, calibrated from each intersection's field data to reflect its driving populations' behavioral characteristics associated with the response to the yellow phase.

Table 4-2: Parameters of Logit model 2 calibrated from each intersection's field data

Site	β_0	β_E	Sample size
MD 4 at Forestville	3.94	-0.85	346
US 301 at Billingsley	6.07	-1.56	138
US 301 at Governor Bridge	5.14	-1.10	135

Computing Type-II dilemma zone

With the assumption that a driver's response to a yellow phase can be reliably predicted with the calibrated behavioral model, one can identify the Type-II dilemma zone at each intersection based on the roadway segment within which a driver's probability of taking the "stop" action when encountering a yellow phase may range from 10-90%. More specifically, most drivers at the upper bound of the identified dilemma zone should have a 90% probability of pressing the brake and taking the stop action when seeing the yellow phase. In contract, those at the lower bound of the dilemma zone, due to its short distance to the intersection, will most likely accelerate through the intersection; only 10% of drivers under such a scenario will decide to stop the vehicle.

Table 4-3: The computed dilemma zone for each candidate intersection based on its own behavioral parameters and Logit model 2

Site	Lower bound (time to the stop bar)	Upper bound (time to the stop bar)
MD 4 at Forestville	2.2 seconds	6.7 seconds
US 301 at Billingsley	2.5 seconds	5.3 seconds
US 301 at Governor Bridge	2.6 seconds	6.6 seconds

4.4 Pre-deployment assessment with simulation experiments

Figure 4-16 illustrates the interrelations between key components of the finalized intersection simulator for experimental analysis, including the system's key control modules, its

operational relations with the signal controller, traffic sensors, and output for performance assessment. Note that prior to the execution of the control module for either simulation experiments or field deployment, those key parameters embedded in its two algorithms must first calibrate with field data to capture the actual behaviors of the target intersection's driving populations. An extensive discussion of those parameters' mathematical properties has been presented in Chapter 3, and its calibration procedure with the field driver behavioral data is described in detail in Figure 4-17.

To assess the safety improvement under each candidate control strategy and its resulting impacts on the signal efficiency, the pre-deployment evaluation is based on potential collisions and the total intersection delay. While the latter is readily available from the output of each simulated traffic scenario, the former must be computed with SSAM (Gettman and Head, 2003a, 2003b; Gettman et al., 2008; FHWA, 2008). The entire assessment, with simulation experiments, consists of the following primary steps:

- Select the state-of-the-practice strategy for actuated signal control as the baseline for effectiveness assessment of the two control algorithms embedded in the control module of the proposed integrated intelligent intersection control system;
- Execute the simulator with the field data and average the output data from multiple replications;
- Take the trajectory records associated with each individual vehicle approaching the target intersection from the simulator's output;
- Import the output of the traffic simulator to SSAM to compute the number of near conflicts for rear-end collisions and angled crashes; and
- Apply the empirical formulation available from SSAM to estimate the projected rear-end collisions in the time span of one year.

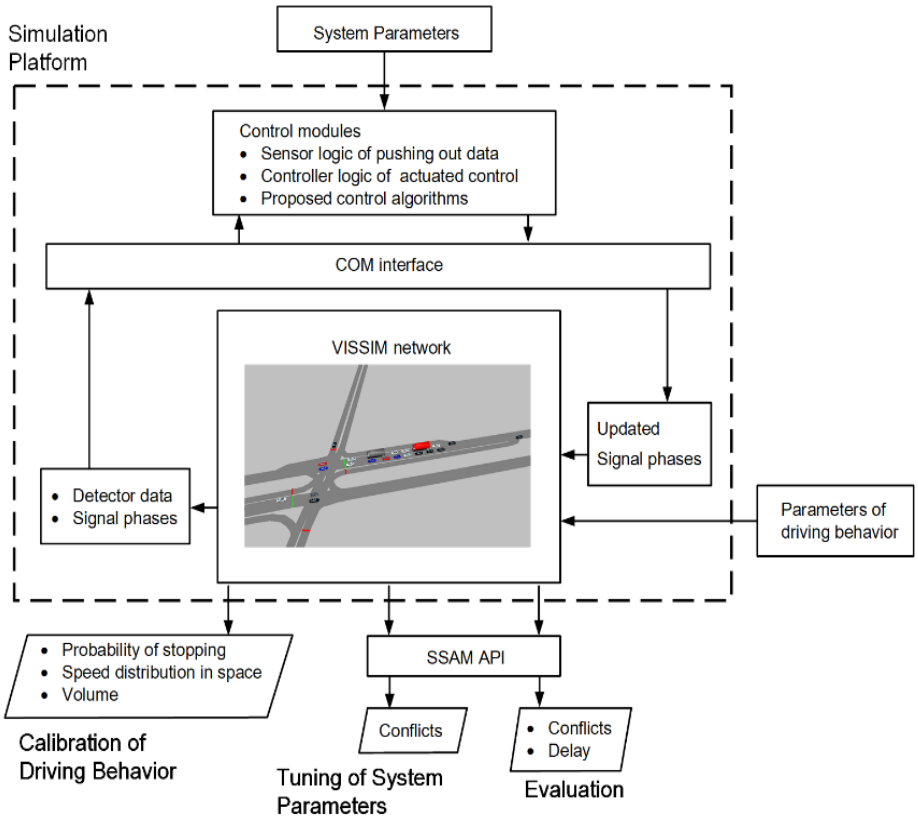

Figure 4-16: Interrelations between the proposed system's key components and their data flows replicated in a real-time intersection actuated control simulator.

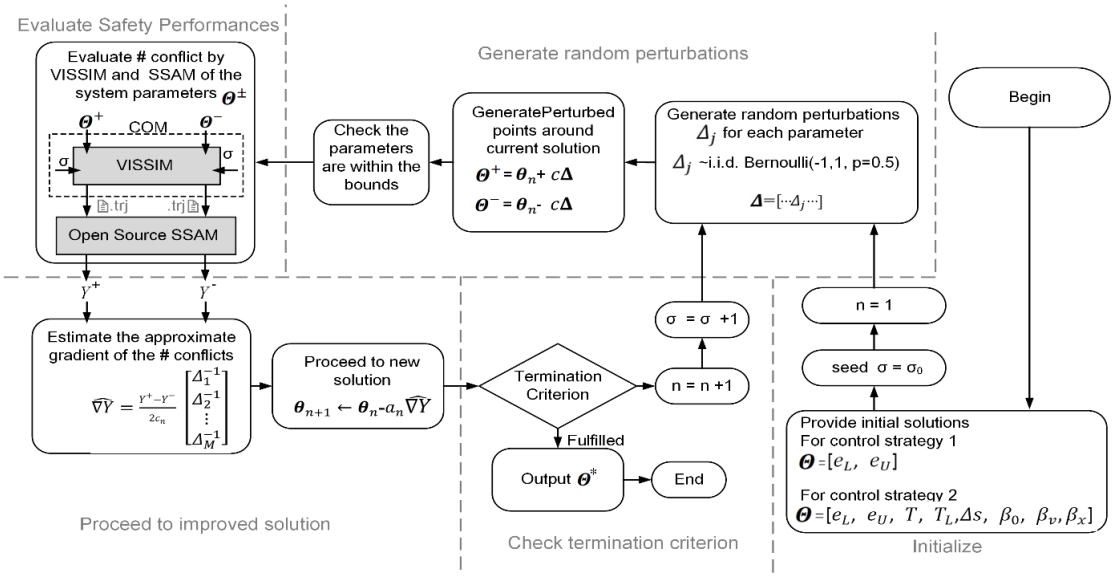

Figure 4-17: Graphical illustration of the procedures for calibrating the key parameters embedded in the proposed system's control algorithms.

4.5 Performance assessment from the simulation results

The pre-deployment performance assessment with simulation analyses is based mainly on the following measures of effectiveness (MOEs):

- Number of vehicles trapped in the dilemma zone under two different control strategies;
- Average delay per vehicle over each candidate intersection under two different control strategies;
- Predicted number of rear-end collisions per year with the two different control strategies; and
- The estimated number of angled conflicts that may result in angled crashes under two different control strategies.

The first two MOEs were measured directly from the output of each candidate intersection's simulator with different time-of-day volumes under the two control strategies for performance comparisons. The computation of the remaining two MOEs, however, must first transfer the vehicle trajectory data from the simulation output to SSAM (FHWA, 2008) and then execute its embedded empirical models to produce the estimates. Figure 4-18 shows an example of the traffic simulator for the intersection of MD 4 @ Forestville Rd. for performing simulation experiments.

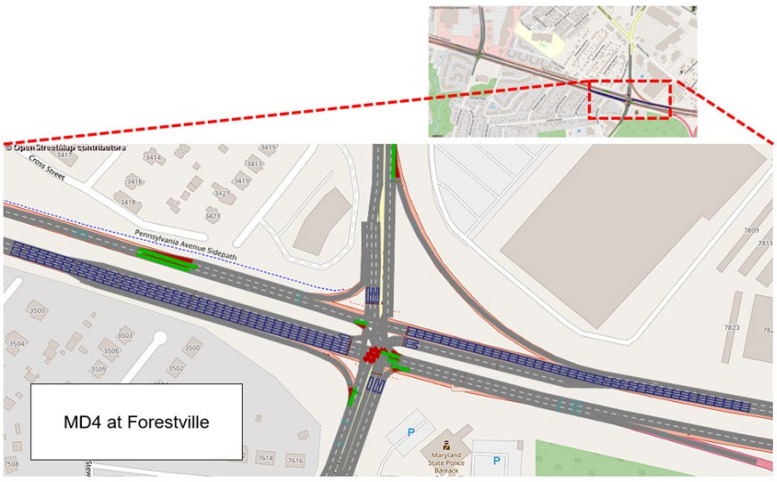

Figure 4-18: The traffic simulator for the intersection of MD 4 @ Forestville Rd. for performing simulation experiments.

Note that since Algorithm 2 outperforms Algorithm 1 with respect to all safety MOEs in the extensive off-line evaluations, only the former is programmed to the III-CS for pre-deployment simulation analyses.

Table 4-4 summarizes the statistics of vehicles trapped in the dilemma zone under the baseline and proposed control strategies at three candidate intersections from the results of extensive simulation experiments. Seemingly, the control strategy adopted by III-CS, compared with the base-line actuated control, can effectively reduce the number of vehicles trapped in the dilemma zone during the yellow phase at all three candidate intersections.

Note that such a statistic is the most direct MOE for assessing the risk level of incurring rear-end collisions at intersections, despite the statistics of predicted rear-end collisions (see Table 4-5), based on the popular software SSAM (FHWA, 2008), do not seem to yield statistically significant improvement. This is likely due to the nature of empirical equations employed by SSAM, which mainly provides an approximated estimate, and are not specially calibrated for the target local intersections with a small probability of occurrence.

Table 4-6 presents the estimated conflicts for potential angled crashes per hour by the two different control strategies at three candidate locations with extensive simulation experiments, revealing the likely reduction of 0% in such conflicts at the intersection of MD 4 @ Forestville Rd., 5.9% at the intersection of US 301@Billingsley Rd., and 3.9% at the intersection of US 301@Governor Bridge when deployed with the III-CS.

Most importantly, the results of extensive simulations at the three intersections seem to support the assertion that the proposed III-CS's execution of rigorous control actions to improve the safety of traffic flows will not be at the expense of excessive intersection vehicle delay. This is evident from the statistics of average delay per vehicle over the three candidate intersections (see Table 4-7), where the resulting differences between the state-of-the-practice control and the proposed III-CS are all around the negligible range of 1%.

Table 4-4: Number of vehicles trapped in the dilemma zone from the simulation results

	MD 4@Forestville	US 301@Billingsley	US 301@Governor Bridge
Baseline control	46.4 veh/hr	18.8 veh/hr	121.8 veh/hr
III-CS-control	17.4 veh/hr	8.6 veh/hr	112.8 veh/hr
Difference	(-62.5%)	(-54.3%)	(-7.4%)

Table 4-5: Estimated rear-end collisions per year* from the simulation results

	MD 4@Forestville	US 301@Billingsley	US 301@Governor Bridge
Baseline control	7.0	6.0	7.60
III-CS-control	7.4	5.2	7.53
Difference	(+5.7%)	(-13.3%)	(-0.9%)

*Estimated with SSAM (FHWA, 2008) from the simulation output

Table 4-6: Estimated angled conflicts for potential crashes from the simulation results

	MD 4@Forestville	US 301@Billingsley	US 301@Governor Bridge
Baseline control	0.2/hr	3.4/hr	20.6/hr
III-CS-control	0.2/hr	3.2/hr	19.8/hr
Difference	(0.0 %)	(-5.9%)	(-3.9%)

*Estimated with SSAM (FHWA, 2008) from the simulation output

Table 4-7: Estimated delay per vehicle from the simulation results

	MD 4@Forestville	US 301@Billingsley	US 301@Governor Bridge
Baseline control	43.2 sec/veh	52.6 sec/veh	21.4 sec/veh
III-CS-control	43.7 sec/veh	52.7 sec/veh	21.6 sec/veh
Difference	(+1.1 %)	(+0.19%)	(+0.9%)

*Computed directly from five replications of the simulation output

4.6 Summary of research findings

This chapter has presented the results of pre-deployment assessment with respect to the proposed III-CS's effectiveness in minimizing rear-end collisions. Based on the field data of key traffic characteristics collected at each candidate intersection and its customized simulator with rigorously calibrated behavioral parameters, this study has conducted extensive simulation experiments, and evaluated the deployed control strategy's effectiveness in reducing the average

number of vehicles trapped in the dilemma zone during the yellow phase, the estimated angle conflicts for potential crashes, the average delay per vehicle, and the projected rear-end collisions. The overall statistics with respect to these four MOEs convincingly support the effectiveness of the proposed III-CS in minimizing the likelihood of rear-end collisions in the green-termination process under the actuated control environment for intersection signal. Moreover, the simulation results from various traffic scenarios also reveal that such safety improvements will not be at the expense of increasing the vehicles' signal delay.

Chapter 5: After-deployment analysis of the III-CS effectiveness on safety improvement

5.1 Introduction of the after-deployment analysis

Due to the impact of the COVID-19 pandemic on the deployment budget and schedule, this study has only deployed the developed III-CS at the intersection of MD 4 @ Forestville Rd. The first after-deployment field observations were conducted in Jan 2021, about one month after the full operation of the deployed III-CS, and the second identical field assessment was completed in March 2021. Both after-deployment field studies and data collection are focused on the III-CS's effectiveness with respect to its three primary functions:

- Timely activation of its dynamic all-red extension function to prevent angled crashes;
- Dynamic extension of the green phase to minimize the number of vehicles trapped in the dilemma zone during the yellow phase; and
- Potential long-term impacts on the behaviors of driving populations, especially in reducing the number of high-speed drivers and red-light runners.

In addition to the before-and-after assessment, the measures of effectiveness (MOE) for the III-CS's performance evaluation collected in two different after-periods will also be compared to assess its potential time-varying impacts on the traffic patterns and the resulting effectiveness.

Table 5-1 summarizes the volume distributions at the intersection of MD 4 @ Forestville Rd. collected before and after the deployment in both peak and off-peak periods, including the average and variance of its approaching traffic speeds monitored by the III-CS's wide-range sensors. Notably, traffic flows seem to maintain the same speed distribution patterns after the deployment, despite the fact that after-deployment volumes, collected in two field studies during the COVID-impact period, are much lower than in the pre-deployment period.

To best understand the impacts of all III-CS's functions on the traffic safety and the behaviors of driving populations, the effective assessment will first focus on the performance of its dynamic all-red extension (DARE) with respect to preventing angled crashes, followed by an in-depth analysis of the functions offered by the dynamic-green-extension (DGE) module in terms

of making the optimal green extension/termination decision. The collective impacts of the III-CS's functions on the driving population's behaviors, and the resulting traffic characteristics, will also be reported in detail.

Table 5-1: Traffic speeds and volumes before and after the deployment

	Before	**After-deployment**	
		1st survey	**2nd survey**
Date	Apri-10-2019	Jan-28-2021	Mar-22-2021
Approach speed [1]			
Mean [mph]	40.9	44.1	42.6
Standard Deviation[mph]	11.1	7.35	7.88
85th-percentile[mph]	51.1	51.0	49.0
Approach Volume [2]	2,133	1,628	1,803
Morning peak[veh/h]	1,999	905	1,198
Morning midday hours[veh/h]	1,683	1,312	1,343
Afternoon midday hours[veh/h]	2,111	1,839	2,044
Evening peak[veh/h]	3,449	2,397	3,157

[1] Approach speed sampled at 800ft upstream of the stop line

[2] Average between 8 AM – 4 PM; eastbound approach only.

5.2 Assessing the effectiveness of the III-CS's dynamic all-red function

All key parameters associated with dynamic-all-red-extension (DARE) at the intersection of MD 4 @ Forestville Rd. are listed below:

- Yellow phase = 5 seconds
- Fixed AR = 3 seconds
- Extensible AR = 0 to 3 seconds
- AR unit extension: 1 second

Note that the DARE is viewed as functioning effectively only if it is activated by the controller when a red-light-running violation occurs during the period of *2.0 (sec) after the onset*

of the red phase (see Figure 5-1). Hence, the system will not activate the DARE if the red-light-running through the intersection takes place during the preset all-red phase.

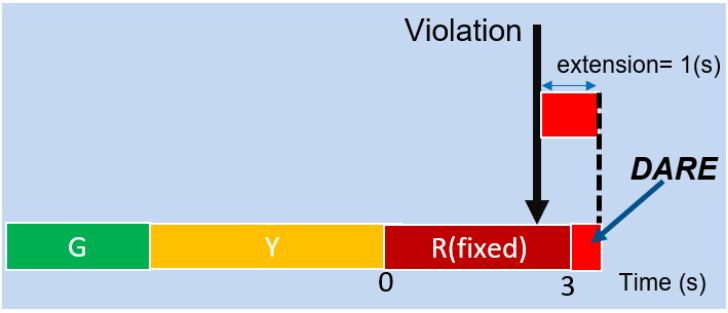

Figure 5-1: Graphical illustration of the DARE's function.

Tables 5-2 summarizes the key statistics for assessing the effectiveness of III-CS's DARE function, including the detection rate, false alarm rate, missed call rate, and the number of red-light-running vehicles per cycle.

As shown in the 1st field survey's statistics, a total of eight red-light-running vehicles were observed during the period of 123 signal cycles; when 3 of those violations took place 2 seconds after the onset of the red phase, the system correctly activated the DARE in time for all such vehicles, and achieved the detection rate of 100 % (i.e., 3 out of 3). However, over the entire observation period, the system activated an additional 9 times of unjustified DARE extensions, resulting in a false alarm rate of 7.3% (9/123) per cycle.

In a similar pattern, the statistics computed from the 2nd field survey data of 196 signal cycles show that the system correctly identified all 7 out of 24 red-light-running vehicles and activated the DARE in time to accomplish a detection rate of 100%. To ensure that a perfect detection rate will inevitably result in some expected false alarms, as reflected in its 11.7% (23/196) of unwarranted extensions per cycle over the observation period.

With respect to the impacts of such a system on the behaviors of driving populations, it is well recognized that more field observations over a longer time period will be needed to evaluate the resulting significance. However, the data reported in Table 5-2 seems to reveal that the intersection selected for system deployment is indeed a high-risk intersection, as reflected in the 8

and 24 red-light running vehicles during the two short periods of field observations. Also, despite the need to conduct more and longer field assessments, the average number of red-light running vehicles per cycle has reduced from the before-period of 0.119 to 0.063 and 0.116, respectively, in the two after-periods. Figure 5-2 illustrates the III-CS's function for identifying red-light running vehicles during the red phase, and Figure 5-3 shows an example of the red phase countdown from the signal controller's screen.

Table 5-2: Before-and-after assessment of DARE's effectiveness

	Before	**After**	
		1st	**2nd**
Date	Apri-10-2019	Jan-28-2021	Mar-22-2021
Number of cycles	92	123	196
Red-light Runnings			
Number of RLR	11	8	24
RLRs occurred at 2.0 (sec) over the onset of red	2	3	7
RLR/cycle	0.119	0.065	0.116
DARE Activation			
# AR-Extension actions	N/A	12	30
# False alarm	N/A	9	23
# Missed call	N/A	0	0
Missed call rate (%)	**N/A**	**0% (0/3)**	**0% (0/7)**
Detection rate (%)	**N/A**	**100% (3/3)**	**100% (7/7)**
False alarm rate (%)[b] (# false alarms/cycle)	**N/A**	**7.3% (9/123)**	**11.7% (23/196)**

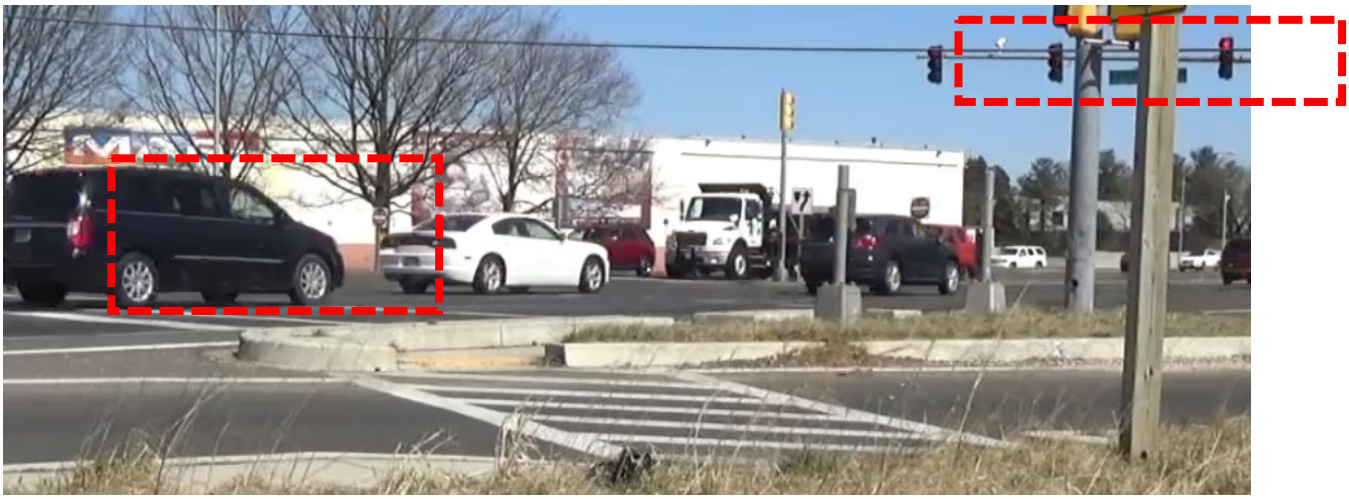

Figure 5-2: The video footage for identifying red-light runners during the red phase.

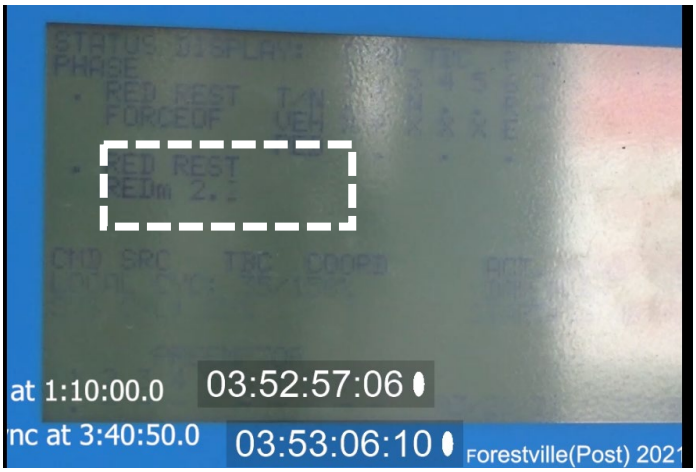

Figure 5-3: The video footage for red phase countdown from the controller's screen.

Table 5-3 shows the performance comparison with respect to the DARE's effectiveness offered by the III-CS and the system with only DARE. Although the DARE's algorithm in the newly developed III-CS is identical to those deployed previously at US 40 and MD 213 intersections (Park et al., 2018), it achieves the same perfect detection rate but a substantially reduced false-alarm rate. This is likely due to the supplemental functions provided by the III-CS's dynamic green extension module, because drivers are less likely to be trapped in the dilemma zone and pressured to take the risk of running over the intersection during the red phase.

Table 5-3: Performance comparison between the DARE in the III-CS and its stand-alone system

	MD 4 [a] **(newly-deployed)**	**US 40 (Park et al.,2018)**	**MD 213 (Park et al.,2018)**
Number of through lanes on major approaches	6	4	2
False alarm rate (%) (#FalseAlarm/#cycle)	10.0% (32/319)	30.0%	16.0%

5.3 Assessing the III-CS's dynamic green-extension (DGE) function

Assessing the effectiveness of the III-CS's DGE function is a relatively challenging task, as it involves the collection of sufficient and reliable data to compute the following information for the selected MOEs:

- *N-activation*: The number of times III-CS activated its DGE function to make the decision of extending the green duration during the sampling period of 0.1 second per interval.
- *N-optimal activation:* The number of times that decisions by the DGE (i.e., either extension or not) indeed resulted in a lower collision risk over the subsequent intervals based on the traffic conditions and the number of vehicles in the dilemma zone.
- *N-non-optimal activation:* The number of times that the DGE's decisions did not result in a reduction in the collision risk over the subsequent intervals based on the traffic conditions and the number of vehicles in the dilemma zone.
- *N-incorrect*: The number of times that the DGE failed to extend the green time when the traffic conditions in the dilemma zone at the sample interval needed such an extension.

To ensure that all essential data are properly collected from each sample signal cycle from the deployed III-CS, one shall carefully proceed with a field study using the following steps:

Step 1: Obtain the onset time of each yellow phase from the video aimed at signal phases (see Figure 5-4);

Step 2: Sample multiple intervals of the III-CS's sensor status before the yellow phase (see Figure 5-4);

Step 3: Record the number of vehicles in the dilemma zone and all associated traffic information to compute and record the current risk level; and

Step 4: Record the same information after one second and compute the change in its risk level.

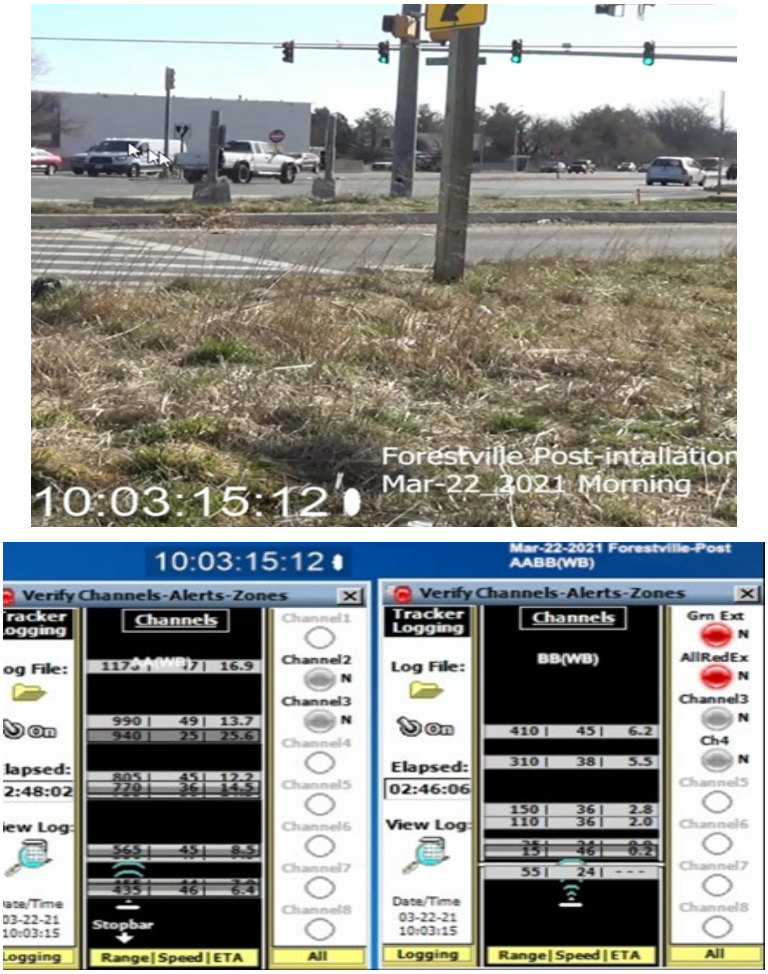

Figure 5-4: Screenshots of video footage for collecting the signal phases and their time with the wide-range sensor.

Table 5-4 summarizes the statistics of the assessment results with respect to the DGE's effectiveness, including the total sample time intervals, the number of DGE activations, the number of optimal and non-optimal DGE activations, and the frequency of missing activations during the two field data collection periods.

Based on the two sets of sample observations collected two months apart, it is noticeable that the DGE modules only made less than 3% (2.7% and 0%) incorrect decisions by not activating the needed green extension. A high reliability offers the best justification for deploying the III-CS with a DGE function. Moreover, the system also made 67% and 81% of optimal decisions, respectively, during the 1st and 2nd field observation periods. Conceivably, the III-CS's DGE was not able to perform as perfectly as desirable, as evidenced in its non-optimal activation rate of 30% and 18.7% during the two observation periods. However, by comparing the DGE's MOEs computed from these two field observations, one may expect that the system's effectiveness is likely to improve over time, because all three MOEs for the system's performance in March 2021 are significantly better than those in January 2021.

The additional measurement with respect to the number of vehicles trapped in the dilemma zone when the DGE activates the green extension also supports its effectiveness, where its average of **2.92** vehicles is much higher than the average of **1.59** vehicles for those intervals not granting a green extension.

Table 5-4: Performance statistics of the III-CS's dynamic green extension

	Short-term Jan-28-2021	Long-term Mar-22-2021
Rate of optimal DGE activation (Number of optimal activations/ Number of activations)	66.7% (72/108) [a]	81.3% (87/107) [a]
Rate of non-optimal activation (N of non-optimal activations/N of activations)	30.6% (33/108)	18.7% (20/107)
Incorrect call rate (Number of incorrect activations/Number of activations)	2.7% (3/108)	0.0% (0/107)

[a] Sample size: 108 and 107 on Jan-28 and Mar 22, respectively. To avoid correlation between samples, samples are at least 1.0 (s) apart, although the signal controller resolution is 0.1 (s;)

5.4 Impacts on the traffic flow characteristics

Table 5-5 presents the comparison statistics of the DGE's potential impacts with respect to the before-and-after traffic characteristics, including the range of the dilemma zones, number of vehicles trapped in the dilemma zone per hour, and deceleration/acceleration rate. Some informative findings critical for future deployment are summarized below:

- Type-II dilemma zone after the system deployment, based on drivers' pass or stop decisions, has been reduced to a narrower range of between 1.7 to 6.2 and 2.1 to 6.2 seconds (i.e., time-to-stop-line) in the 1st and 2nd field observations, respectively, compared to the boundaries of between 2.2 to 6.7 seconds during the pre-deployment period. This is likely due to improved transition timing from the green to the yellow phase that can reduce the risky scenarios of vehicles running through intersections during the yellow or red phases.
- The average number of vehicles trapped in the dilemma zone per hour has reduced from 48.3 veh/hr in the pre-deployment period to 39.7 veh/hr and 39.4 veh/hr, respectively, in the 1st and 2nd field observations. These results show approximately an 18% reduction in one of the direct contributors to an intersection's collision risk.
- The set of deceleration-related statistics for drivers encountering the yellow phase exhibits a significant reduction from the pre-deployment to the system's fully operational period, demonstrating that driving populations after the deployment of the III-CS seem to behave less aggressively over time. For instance, the average deceleration rate of vehicles approaching the intersection during the yellow phase reduced from 3.28 to 2.15 (ft/s^2); so are the trends of the maximum deceleration rate (i.e., 15.4 to 11.0 ft/s^2) and its 85th percentile value (7.06 to 5.73 ft/s^2).
- The spatial distribution of the traffic speeds from the distance of 650 ft (i.e., the upper bound of the sensor's monitoring zone) to the intersection's stop line before and after the deployments, as shown in Figure 5-5, clearly indicate that the presence of an III-CS has

some impact on reducing aggressiveness in the driving population. This results in a relatively slower and smooth speed distribution pattern.

- The III-CS's impact on reducing both the speed and deceleration distributions of vehicles approaching the intersection during the yellow phase offers direct support to the DGE's effectiveness in reducing the risk of rear-end collisions.

Table 5-5: Driving behaviors before and after the field deployment

	Before	**After**	
		1st	**2nd**
Date	Apr-10-2019	Jan-28-2021	Mar-22-2021
Sample Size	328 (veh)	150 (veh)	219 (veh)
Dilemma zone (in terms of estimated time-to-stop line)			
Upper bound (sec) (90% vehicles stopped)	6.7	6.2	6.2
Lower bound (sec) (10% vehicles stopped)	2.2	1.7	2.1
Range (sec)	4.5	4.5	4.1
Number of vehicles trapped in the dilemma zone (veh/h)[a]	48.3	39.7 (-17.9%) [a]	39.4 (-18.5%) [a]
Deceleration rate[b] (ft/s^2)			
Maximum	15.4	11.3	11.0
85% Percentile	7.96	7.18	5.73
Mean (Standard Deviation) [c]	3.28 (4.55)	3.99 (3.34)	2.15 (3.49)

[a] Compared to pre-deployment;
[b] Sampling vehicles that stopped on yellow phases only and between 100 to 550(ft) upstream of the stop line;
[c] Standard deviation might be larger than mean since the distribution is positively skewed.

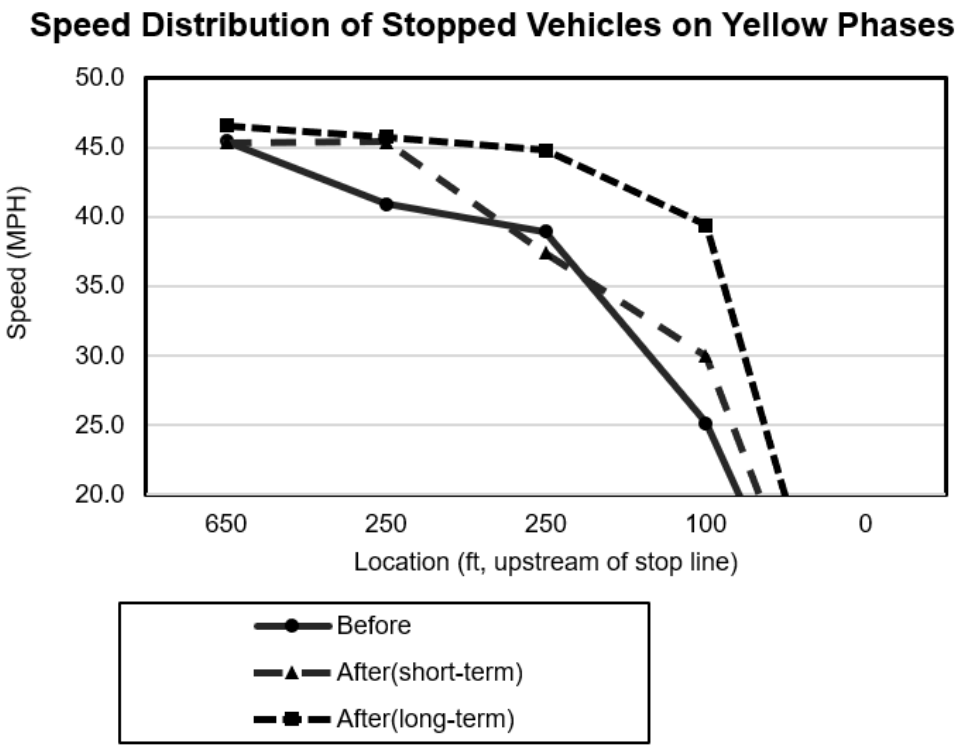

Figure 5-5: Spatial distribution of the traffic speeds before and after the deployment.

5.5 Summary of assessment findings

This chapter has summarized the results of performance assessment with respect to the deployed III-CS's effectiveness in improving traffic safety at high-risk intersections. Based on the data and analysis results from two field studies two months apart, the deployed III-CS has proved its effectiveness in preventing angled crashes with its perfect detection rate, optimally activating or terminating the green extension, and by significantly reducing the number of vehicles trapped in the dilemma zone. These results confirmed the main contributing factors to rear-end collisions.

After recognizing its presence at the intersection by the driving population, the deployed III-CS, with its detection sensors, DGE, and DARE functions, showed an increasingly significant impact on traffic patterns. The results relayed a progressively smoother distribution of the approaching vehicles' speeds and deceleration rates during the yellow phase. The impacts on driving behaviors are also demonstrated in the significant reduction in the average length of the dilemma zones experienced by drivers approaching the target intersection after the deployment.

In summary, although the long-term impacts and effectiveness of the III-CS should be observed over time through more periodical field studies, the system after its three-month deployment has yielded the desirable MOEs as anticipated. The III-CS offered the promise of further deployment and possible extension to integrate with other control measures/systems for safety improvement at both the intersection and arterial levels.

Chapter 6: Conclusions

6.1 Summary of research findings

Most signalized intersections designed for delay minimization often cannot address the safety issues—mainly rear-end collisions and angled crashes—that occur during the phase transitions from green to yellow and yellow to red. After being deployed at multiple intersections over a long period, our previously developed system for the dynamic all-red extension (DARE) has demonstrated its effectiveness in preventing angled crashes due to mostly red-light running. This study has focused on extending its functions with two dynamic green-extension algorithms to tackle the rear-end collision with the same controller, communications hardware, and sensors. Inherently, the entire system, named the integrated intelligent intersection control system (III-CS), comprises three control algorithms, one for dynamic all-red extension and two for dynamic green extension/termination.

The first control algorithm, featuring effectiveness and convenience for application, is mainly to replace the point detector used in the conventional gap-out control for detecting the vehicle presence in the dilemma zone with the wide-range sensor during the phase transition intervals. With a rigorously calibrated dilemma zone from the field data, this algorithm has shown superior performance over the conventional actuated control with respect to reducing the conflicts for potential rear-end collisions, and the number of vehicles trapped in the dilemma zone at three intersections selected for pre-deployment evaluation.

Conversely, the safety function of such a control algorithm may be constrained if the green duration, under some traffic conditions, is extended to the state that meets the criteria for termination. Hence, this study has further proposed a two-stage algorithm that employs the first algorithm in its stage-1 green phase, but terminates the stage-2 green only at the time frame predicted to have the lowest risk of causing rear-end collisions between each pair of leading-following vehicles detected by the sensor. This advanced control algorithm, as expected, has outperformed the first proposed algorithm under various traffic conditions, based on the pre-deployment evaluation with extensive field data and simulation experiments. Hence, it was selected to deploy at the intersection of MD 4 and Forestville Rd.

The results of two extensive field evaluations, conducted one and three months after the III-CS deployment, have convincingly demonstrated its functions in improving most safety related measures of effectiveness at the target intersection. Hence, from both the pre-deployment simulation analyses and before-and-after comparison after deployment, one can summarize the following benefits that can be provided by a rigorously deployed III-CS:

- Decreasing the number of near conflicts that may result in rear-end collisions between vehicles trapped in the dilemma zones during phase transitions;
- Reducing the aggressive level of the driving population with respect to the distribution of their approaching speeds and deceleration/acceleration rate to the intersection;
- Shaping the behaviors of the driving population when they encounter a yellow phase, as reflected in their much lower average and maximum acceleration/deceleration rates during the yellow phase after the III-CS deployment;
- Incentivizing more drivers to choose the stop decision when encountering a yellow phase, and observing fewer drivers that ran through the intersection during the red and all-red phases;
- Type-II dilemma zone, based on drivers' pass or stop decisions, were observed to reduce to a narrower range at the intersection deployed with the III-CS - between 2.1 to 6.2 seconds of time-to-stop-line, shorter than the range of between 2.2 to 6.7 seconds in the pre-deployment period;
- The dynamic green extension function provided by the III-CS not only minimizes the likelihood of incurring rear-end collisions, but also concurrently contributes to a reduction in red-light running as well as the need to activate the all-red extension;
- Offering the real-time available time-varying traffic queue length and its evolution for use as the key information for design of the delay-minimization-based signal plan;
- Reliably activate the dynamic all-red extension functions to prevent angled crashes, although at some level of false alarms; and
- Enabling the responsible traffic engineers to monitor the queue evolution pattern in real time at the target intersection, including the number of vehicles present in the wide-range

sensor's detection zone, and such vehicles' time-varying speeds and times to reach the intersection.

Most importantly, the effective exercise of III-CS's functions to yield the above benefits will not be at the expense of increasing the traffic delay. The developed III-CS's remote monitoring module, with properly calibrated thresholds and per-specified criteria, can provide the functions for congestion monitoring and arterial incident detection.

6.2 Future research works

Although the III-CS has demonstrated its effectiveness in preventing rear-end collisions and angled crashes at high-speed intersections, its focus is mainly on through vehicles on the primary roads and the side traffic; it has not yet tackled those accidents involving turning vehicles. Moreover, a successful deployment of such a system at one intersection, due to its impacts on the behaviors of the driving population, may in turn affect the arriving patterns at downstream intersections. Noticeably, such a change in traffic distribution patterns over an arterial with optimally coordinated signals may significantly impact the progression efficiency and result in excessive delay at some of its intersections without the III-CS. Hence, how to integrate the safety features of the developed III-CS with the state-of-the-practice signal design methods for maximizing traffic flow efficiency over an arterial is an essential task. In addition, to maximize the effectiveness of a deployed III-CS, one may explore its integration with a control strategy of variable speed limit (VSL) to reduce the spatial coverage of the dilemma zone, or extend the system's functions to include a red-light camera. This may concurrently minimize red-light running vehicles, which is another cause of rear-end collisions.

Further studies along this line of improving intersection safety and maximizing arterial flow efficiency shall include the following tasks:

- Deploying the developed III-CS at more intersections with different geometric features and congestion levels to ensure its effectiveness and identify any potential limitations;

- Collecting more after-deployment data to assess the short- and long-term impacts of an III-CS's deployment on the distribution of the target intersection's traffic speeds, drivers' responses during the yellow phase, and the number of aggressive red-light running vehicles;
- Exploring the potential of extending the III-CS's functions to address the crashes between left-turning vehicles and opposing through traffic with minimal additional hardware;
- Investigating the pros and cons of integrating the III-CS with red-light camera for concurrently minimizing the red-light runners and protecting the resulting angled crashes;
- Investigating the optimal integration with the VSL control to reduce the number of vehicles likely to be trapped in the dilemma zone, based on the speed distribution of traffic flow speeds and the congestion level;
- Incorporating the III-CS's safety features in the existing delay-minimization models for signal design to ensure the target intersection can fully utilize all devices used for safety needs or traffic monitoring;
- Researching the impacts of deploying the III-CS at some of the target arterial's intersections on its overall traffic flow patterns and the resulting signal coordination efficiency;
- Developing an efficient methodology for identifying the optimal number of intersections and their locations along an arterial for deploying the III-CS so that the entire arterial can achieve the desirable state of efficiency and safety at the minimal deployment cost;
- Comparing the III-CS's effectiveness with other non-radar sensors (e.g., image sensors) under different traffic conditions and driving populations; and
- Advancing the III-CS's function to include the arterial/intersection incident detection and monitoring based on the time-varying traffic queues and speed information available from its wide-range sensors.

References

1. AASHTO (2010), *Highway Safety Manual*, Washington, DC, USA, 2010

2. Abadi, M. G., Hurwitz, D. S., Marnell, P., & Quayle, S. (2017). Evaluation of red clearance extension designs with hardware-in-the-loop simulation. *Transportation letters*, *11*(5), 264-274.

3. Abbas, M. M., Wang, Q., Higgs, B., Sarabi, D. Z., Machiani, S. G., & Mladenovic, M. N. (2016). High-Resolution Field Evaluation of Radar-Based Dilemma Zone Protection System. *Transportation Research Record*, *2557*(1), 11-23.

4. Archer, J., & Young, W. (2009). Signal treatments to reduce heavy vehicle crash-risk at metropolitan highway intersections. Accident Analysis & Prevention, *41*(3), 404-411.

5. Baguley, C. J., & Ray, S. D. (1989). Behavioural assessment of speed discrimination at traffic signals, TRRL Research Report, 177, Berkshire, U.K.

6. Bhatnagar, S., Prasad, H., & Prashanth, L. (2013). Service Systems. In *Stochastic Recursive Algorithms for Optimization* (pp. 225-241). Springer, London.

7. Bonneson, J. A. & Mccoy P. T. (1996). Traffic Detector Designs for Isolated Intersections. *ITE Journal*, *66*, 42-47.

8. Bonneson, J., Middleton, D., Zimmerman, K., Charara, H., & Abbas, M. (2002). Intelligent detection-control system for rural signalized intersections. *Texas Transp. Inst., College Station, TX, Rep. FHWA/TX-03/4022-2*.

9. Chang, M. S., Messer, C. J., & Santiago, A. J. (1985). Timing traffic signal change intervals based on driver behavior. *Transportation Research Record*, *1027*, 20-30.

10. Chau, M., & Fu, M. C. (2015). An overview of stochastic approximation. In *Handbook of Simulation Optimization* (pp. 149-178). Springer, New York, NY.

11. Chiou, Y. C., & Chang, C. H. (2010). Driver responses to green and red vehicular signal countdown displays: Safety and efficiency aspects. *Accident Analysis & Prevention*, *42*(4), 1057-1065.

12. Elhenawy, M., Jahangiri, A., Rakha, H. A., & El-Shawarby, I. (2015). Modeling driver stop/run behavior at the onset of a yellow indication considering driver run tendency and roadway surface conditions. *Accident Analysis & Prevention*, *83*, 90-100.

13. Federal Highway Administration (FHWA) (2003). Manual on uniform traffic control devices for streets and highways – 2003 Edition, Washington, D.C.

14. Federal Highway Administration (FHWA) (2008). Surrogate Safety Assessment Model (SSAM) Software User Manual, McLean, VA, USA.

15. Federal Highway Administration (FHWA) (2009). Manual on uniform traffic control devices for streets and highways – 2003 Edition, Washington, D.C.

16. Gates, T. J., Noyce, D. A., Laracuente, L., & Nordheim, E. V. (2007). Analysis of driver behavior in dilemma zones at signalized intersections. *Transportation Research Record*, *2030*(1), 29-39.

17. Gazis, D., Herman, R., & Maradudin, A. (1960). The problem of the amber signal light in traffic flow. *Operations Research*, *8*(1), 112-132.

18. Gettman, D., & Head, L. (2003). Surrogate safety measures from traffic simulation models. *Transportation Research Record*, *1840*(1), 104-115.

19. Gettman, D., Pu, L., Sayed, T., Shelby, S., & Siemens, I. T. S. (2008). *Surrogate Safety Assessment Model and Validation* (No. FHWA-HRT-08-051).

20. Hastie, T., Tibshirani, R., & Friedman, J. (2009). *The elements of statistical learning: data mining, inference, and prediction*. Springer Science & Business Media.

21. Hurwitz, D. S., Knodler Jr, M. A., & Nyquist, B. (2011). Evaluation of driver behavior in type II dilemma zones at high-speed signalized intersections. *Journal of Transportation Engineering*, *137*(4), 277-286.

22. Hurwitz, D. S., Wang, H., Knodler Jr, M. A., Ni, D., & Moore, D. (2012). Fuzzy sets to describe driver behavior in the dilemma zone of high-speed signalized intersections. *Transportation Research Part F: Traffic Psychology and Behaviour*, *15*(2), 132-143.

23. Hurwitz, D., Abadi, M. G., McCrea, S., Quayle, S., & Marnell, P. (2016). *Smart red clearance extensions to reduce red-light running crashes* (No. FHWA-OR-RD-16-10). Oregon. Dept. of Transportation.

24. Knodler Jr, M. A., & Hurwitz, D. S. (2009). An evaluation of dilemma zone protection practices for signalized intersection control (No. Report No. 2009-6).

25. Kronborg, P., & Davidsson, F. (1993). MOVA and LHOVRA: traffic signal control for isolated intersections. *Traffic Engineering and Control*, *34*(4), 195-200.

26. Kronborg, P., Davidsson, F., & Edholm, J. (1997). SOS-Self Optimising Signal Control. Transport Research Institute, Stockholm

27. Law, A. M. & W. D Kelton (2000). Simulation Modeling and Analysis, 3rd edition McGraw-Hill: Boston.

28. Li, M., Chen, X., Lin, X., Xu, D., & Wang, Y. (2018). Connected vehicle-based red-light running prediction for adaptive signalized intersections. *Journal of Intelligent Transportation Systems*, *22*(3), 229-243.

29. Liu, Y., Chang, G. L., & Yu, J. (2012). Empirical study of driver responses during the yellow signal phase at six Maryland intersections. *Journal of Transportation Engineering*, *138*(1), 31-42.

30. Maryland State Police. (Dec. 2019). Maryland Statewide Vehicle Crashes [Online] Available: https://opendata.maryland.gov/Public-Safety/Maryland-Statewide-Vehicle-Crashes/65du-s3qu

31. National Highway Traffic Safety Administration (NHTSA) (2009). Novice Teen Driver Education and Training Administrative Standards. Washington, DC: National Highway Traffic Safety Administration

32. National Highway Traffic Safety Administration (NHTSA), (2019). "Traffic Safety Facts 2017 - A Compilation of Motor Vehicle Crash Data" Washington, DC, USA, DOT HS 812 806

33. NGSIM (2017). Open Source SSAM Computation Engine API. Florence, KY. 2017

34. Olson, C. S. (2012). Safety Effectiveness of Red-Light Treatments for Red Light Running. Master Thesis.

35. Ozbay, K., Yang, H., Bartin, B., & Mudigonda, S. (2008). Derivation and validation of new simulation-based surrogate safety measure. *Transportation Research Record*, 2083(1), 105-113.

36. Papaioannou, P. (2007). Driver behaviour, dilemma zone and safety effects at urban signalised intersections in Greece. *Accident Analysis & Prevention*, *39*(1), 147-158.

37. Park, S. Y., Lan, C. L., Chang, G. L., Tolani, D., & Huang, P. (2016). Design and pre-deployment assessment of an integrated intersection dilemma zone protection system. *Journal of Transportation Engineering*, *142*(12), 04016063.

38. Park, S. Y., Lan, C. L., Rao, R. S., & Chang, G. L. (2018). Field evaluation of the dilemma zone protection system at suburban intersections. *Transportation Research Record*, *2672*(21), 51-62.

39. Parsonson, P. S., Roseveare, R. W., & Thomas Jr, J. R. (1974). Small-area detection at intersection approaches. *Traffic engineering*, *44*(Tech Rept).

40. Parsonson, P. S., Day, R. A., Gawlas, J. A., & Black, G. W. (1979). Use of EC-DC detector for signalization of high-speed intersections. *Transportation Research Record*, *737*, 17-23.

41. Peterson, A., Bergh, T., & Steen, K. (1986). LHOVRA—a new traffic signal control strategy for isolated junctions. *Traffic Engineering & Control*, *27*(7-8), 388-389.

42. Savolainen, P. T., Sharma, A., & Gates, T. J. (2016). Driver decision-making in the dilemma zone–Examining the influences of clearance intervals, enforcement cameras and the provision of advance warning through a panel data random parameters probit model. *Accident Analysis & Prevention*, *96*, 351-360.

43. Sharma, A., Bullock, D. M., & Peeta, S. (2007). Recasting dilemma zone design as a marginal cost–benefit problem. *Transportation Research Record*, *2035*(1), 88-96.

44. Sharma, A., Bullock, D., & Peeta, S. (2011). Estimating dilemma zone hazard function at high-speed isolated intersection. *Transportation Research Part C: Emerging Technologies*, *19*(3), 400-412.

45. Simpson, C. L., Harrison, M. W., & Troy, S. A. (2017). Implementation of a Dynamic All-Red Extension at Signalized Intersections in North Carolina: Evaluation of Driver Adaptation and Operational Performance. *Transportation Research Record*, 2624(1)

46. Souleyrette, R. R., O'Brien, M. M., McDonald, T., Preston, H., & Storm, R. (2004). Effectiveness of all-red clearance interval on intersection crashes (No. MN/RC-2004-26,).

47. Spall, J. C. (1992). Multivariate stochastic approximation using a simultaneous perturbation gradient approximation. *IEEE Transactions on Automatic Control*, *37*(3), 332-341.

48. Sheffi, Y., & Mahmassani, H. (1981). A model of driver behavior at high-speed signalized intersections. *Transportation Science*, *15*(1), 50-61.

49. Tarko, A., Li, W., & Laracuente, L. (2006). Probabilistic approach to controlling dilemma occurrence at signalized intersections. *Transportation research record*, *1973*(1), 55-63.

50. Urbanik, T., & Koonce, P. (2007). The dilemma with dilemma zones. *Proceedings of ITE District, 6.*

51. Vincent, R. A., & Peirce, J. R. (1988). *'MOVA': Traffic Responsive, Self-optimising Signal Control for Isolated Intersections*. Traffic Management Division, Traffic Group, Transport and Road Research Laboratory.

52. Wang, X., & Abdel-Aty, M. (2007). Right-angle crash occurrence at signalized intersections. *Transportation Research Record*, *2019*(1), 156-168.

53. Wavetronix (2016). Smart sensor advance user guide Wavetronix LLC.

54. Webster, F. & P. Ellson (1965). Traffic signals for high-speed roads, Road Research Laboratory, Berkshire, UK. Technical Paper No. 74. 1965

55. Wood, J., & Donnell, E. T. (2016). Safety evaluation of continuous green T intersections: A propensity scores-genetic matching-potential outcomes approach. *Accident Analysis & Prevention*, *93*, 1-13.

56. Zegeer, C. V. & R. C. Deen (1978). Green-extension systems at high-speed intersections. *ITE Journal*, *48*(11), 19-24.

57. Zimmerman, K. (2007). Additional dilemma zone protection for trucks at high-speed signalized intersections. *Transportation research record*, *2009*(1), 82-88.

58. Zimmerman, K., & Bonneson, J. A. (2004). Intersection safety at high-speed signalized intersections: Number of vehicles in dilemma zone as potential measure. *Transportation Research Record*, *1897*(1), 126-133.

59. Zimmerman, K., Tolani, D., Xu, R., Qian, T., & Huang, P. (2012). Detection, control, and warning system for mitigating dilemma zone problem. *Transportation research record*, *2298*(1), 30-37.

60. Zhang, L., Zhou, K., Zhang, W. B., & Misener, J. A. (2011). Dynamic all-red extension at signalized intersection: probabilistic modeling and algorithm (No. UCB-ITS-PWP-2011-01). Partners for Advanced Transit and Highways (PATH).

61. Zhang, L., Wang, L., Zhou, K., & Zhang, W. B. (2012). Dynamic all-red extension at a signalized intersection: a framework of probabilistic modeling and performance evaluation. *IEEE Transactions on Intelligent Transportation Systems*, *13*(1), 166-179.